Coordination Chemistry Reviews 254 (2010) 2519–2532

Contents lists available at ScienceDirect

Coordination Chemistry Reviews

journal homepage: www.elsevier.com/locate/ccr

Review

# Photoinduced rearrangements in transition metal compounds

Johannes G. Vos*, Mary T. Pryce

*Solar Energy Conversion SRC, School of Chemical Sciences, Dublin City University, Glasnevin, Dublin 9, Ireland*

**Contents**

1. Introduction ..... 2519
2. Photoinduced ligand exchange ..... 2520
3. Photoinduced isomerisation within the coordination sphere ..... 2522
4. Photoinduced linkage isomerisation/chelate formation ..... 2522
5. Photoinduced *cis–trans* rearrangements ..... 2525
6. Concluding remarks and future developments ..... 2530
Acknowledgements ..... 2531
References ..... 2531

ARTICLE INFO

*Article history:*
Received 4 February 2010
Accepted 12 April 2010
Available online 18 April 2010

*Keywords:*
Photochemistry
Transition metal
Organometallic
Isomerisation rearrangements
Photocatalytic

ABSTRACT

In this contribution a range of photoinduced ligand rearrangements observed for the 1st and 2nd row transition metal and organometallic compounds are discussed. The processes discussed include photoinduced ligand exchange, linkage isomerisation and changes occurring within the coordination sphere of the compounds such as *cis–trans* and *fac–mer* isomerisations. The relevance of these processes for photocatalytic cycles or their application as synthetic tools is discussed where appropriate.



## 1. Introduction

From the early work of Adamson and co-workers [1,2] the investigation of the photoinduced properties of transition metal and organometallic compounds has developed strongly over the last 50 years. While early studies were mainly concerned with the 1st row transition metals, the last 30 years have targeted complexes of the 2nd and 3rd row transition metals. Investigations centred on the 2nd and 3rd row elements were to a large extent driven by the realisation that based on their photophysical properties, ruthenium polypyridyl complexes are potential photocatalysts for the splitting of water by sunlight [3]. As a result, extensive studies on the photostability of these compounds were carried out and since the late seventies the number of studies of the photophysical properties of the 2nd and 3rd row transition metal complexes has expanded significantly [4]. Research in this area was further intensified when the application of ruthenium polypyridyl in dye-sensitised solar cells was reported [5]. A wide range of mononuclear and multinuclear metal ruthenium complexes have been prepared and their photophysical and electrochemical properties, which are essential to their potential applications, have been investigated in great detail. Investigations of the electrochemical and excited state properties of ruthenium complexes have also indirectly lead to a widening the research on complexes based on metals such as Ir and Re [6]. In addition, a wide range of applications have been realised with metal complexes being applied as electrochemically driven sensors for analytes such as glucose, nitrite, nitrate and ascorbic acid [7] and in molecular electronics [8]. Photonically driven developments include applications such as oxygen sensors [9], OLEDS [10], molecular wires [11], bioprobes for biomolecules [12,13] and molecular machines such as motors and switches [11]. The work of Gust and co-workers [14] on a biomimetic model for ATP synthase has been inspirational and has led to the study of photoinduced molecular motion and the development of molecular machines. The work of Feringa and co-workers [15] on mono-directional molecular motors driven based on a biphenanthrylidine compound constituted a prime example of how the combination of light-driven and thermal stimuli

* Corresponding author. Tel.: +353 1 7005307; fax: +353 1 7005503.
*E-mail address:* han.vos@dcu.ie (J.G. Vos).

0010-8545/$ – see front matter © 2010 Elsevier B.V. All rights reserved.
doi:10.1016/j.ccr.2010.04.010

can be harnessed to develop molecular machines. In the transition metal area the elegant studies of a number of groups on the photoinduced and electrochemically driven mobility of catenanes and rotaxanes had a considerable influence on the study of photoinduced mobility [16]. Finally, with the increasing importance of energy issues, the development of sustainable and environmentally friendly energy sources is rapidly growing with issues such as photocatalytic hydrogen [17] or oxygen [18] generation and $CO_2$ reduction [19] attracting much attention.

Metal carbonyl compounds have found widespread use in organic syntheses and catalytic industrial processes [20]. The advantage of metal carbonyls is the efficiency with which the carbonyl ligands may dissociate under either thermal or photo-excitation. In recent years the use of metal carbonyls in photochromic materials has been investigated. Photochromic molecules have potential use as memory devices or optical switches. Systems incorporating metals to photo-switchable dithienylethenes are seen as the next generation of photoresponsive materials [21]. Photoisomerisation of alkenes is one of the most thoroughly studied photochemical reactions, and photoisomerisable molecules have been demonstrated to be exceptionally versatile systems in molecular devices, such as molecular switches, unidirectional molecular motors and in optical information storage [22]. Coordination of stilbene type ligands to transition metals makes it possible to trigger isomerisation with low energy photons via excitation of the MLCT transition.

For many of the light-driven device processes a fundamental understanding of the photochemical behaviour of all components is of prime importance. Properties such as the stability of metal complexes under irradiation, the nature of photoinduced intermediates and the mechanisms leading to photoinitiated ligand loss, ligand isomerisation and rearrangements, are photochemical processes that are central to the design of molecular devices and photocatalysts. In this contribution an overview of photoinduced changes within the coordination sphere of transition metal and organometallic compounds is presented. Particular attention will be paid to photoisomerisations and photoinduced ligand rearrangements that can be reversed photonically or thermally. The importance of these processes for photo-driven applications will be discussed as well as the application of photoinduced ligand rearrangements as a synthetic tool. The catenane and rotaxane areas have recently been reviewed extensively [16] and are not discussed in any detail in this overview. A number of other reviews relevant to photoinduced processes have been published in the last years [23].

## 2. Photoinduced ligand exchange

Photoinduced ligand exchange is one of the most basic photochemical reactions and is essential to most of the processes discussed in this overview. For transition metal complexes ligand exchange is associated with the breaking of metal–ligand bonds. Therefore, the photolability of compounds is generally associated with the presence of antibonding metal centred orbitals. An energy diagram typical for ruthenium polypyridyl complexes is shown in Fig. 1, outlining the energy levels involved in photochemical processes. In this type of compound excitation from the metal-based ground state to a singlet metal-to-ligand charge-transfer state ($^1$MLCT) and fast picosecond intersystem crossing lead to population of a relatively long lived $^3$MLCT state (triplet metal-to-ligand charge-transfer). The detailed work of Meyer and co-workers on ruthenium polypyridyl complexes has identified the $^3$MC (metal centred) orbital as being responsible for the photocomposition observed [24]. For photoactive compounds population of the antibonding $^3$MC state from the $^3$MLCT state takes place at room temperature and the photolability of the complexes is generally

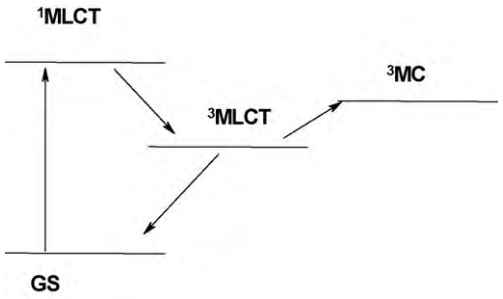


**Fig. 1.** Electronic levels in $[Ru(bpy)_3]^{2+}$.

related to the energy difference between the deactivating $^3$MC state and the emitting $^3$MLCT level (see Fig. 1).

Meyer and co-workers observed that such photoprocesses may also be strongly dependent on the solvent used. Strong ligands such as acetonitrile and also coordinating counter ions can increase the quantum yield for ligand loss. So while $[Ru(bpy)_3](PF_6)_2$ shows little or no decomposition in $CH_2Cl_2$, in the presence of $Cl^-$ or $NCS^-$ ions, formation of species such as $[Ru(bpy)_2Cl_2]$ is observed. The photolability of $[Ru(bpy)_3](PF_6)_2$ is much increased in coordinating solvents such as acetonitrile and bpy loss may be observed [24]. The formation of intermediates containing monodentate coordinated bpy ligands has been observed using $^1$H NMR [25] coupled with electronic spectroscopy.

The photophysical and photochemical behaviour of many other polypyridyl compounds has been studied in great detail. As expected, complexes with monodentate ligands will be more photolabile but this lability depends on the type of ligands and the solvent used. The compound $[Ru(bpy)_2(CO)Cl]^+$ is considered here as an example. This compound is obtained as a side product in the synthesis of $[Ru(bpy)_2Cl_2]\cdot 2H_2O$, the main starting material for ruthenium polypyridyl complexes [26]. The amount of this species formed may be considerable, especially with long reaction times, where decomposition of DMF, which is used as a solvent becomes important. However, the compound can itself be used as an excellent starting material especially when compounds of the type $[Ru(bpy)_2LCl]^+$ or $[Ru(bpy)_2(CO)L]^{2+}$ are required [27]. Different types of ligand L can be introduced by using either thermal or photochemical methods. For example the $Cl^-$ anion can be removed thermally and replaced by ligands such as $NCS^-$, $H^-$, $H_2O$, $CH_3CN$ and pyridine. Importantly, the CO group is not exchanged in the thermal process. However, when the compound is photolysed with UV light in organic solvents, the CO ligand is effectively replaced and $[Ru(bpy)_2LCl]^+$ type complexes, where L is $H_2O$, $CH_3CN$ or pyridine can be obtained. Interestingly the related complex $[Ru(bpy)_2(CO)H]^+$ is considerably more photostable [28]. Importantly, compounds of this type have been proposed as catalysts in the light-driven [29] and electrochemical [30] reduction of $CO_2$ and as intermediates in the water gas shift reaction [31]. Consequently their photochemical and thermal properties with respect to ligand loss are of interest. The results discussed above show that for the monocarbonyl compounds, CO loss is not observed under thermal conditions and this is an important observation for the water gas shift reaction which is thermally driven. In addition the stability of the compounds under visible irradiation allows for their application, in combination with photosensitisers such as $[Ru(bpy)_3]^{2+}$, as photocatalysts for the reduction of $CO_2$ [29].

Other examples of ligand loss have been observed for compounds such as $[Ru(bpy)_2(4\text{-vinylimidazole})Cl]^+$ [32]. Upon photolysis in acetonitrile the imidazole ligand is exchanged, forming $[Ru((bpy)_2(CH_3CN)Cl]^+$ while in methanol the chloride ion is

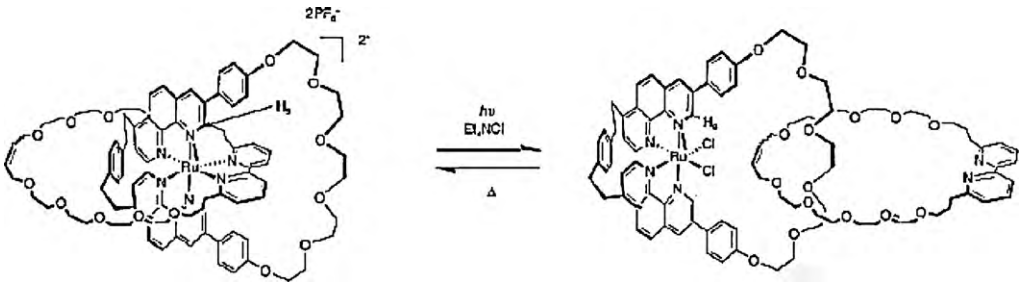

**Fig. 2.** Photochemical and thermal rearrangement for a ruthenium catenane complex.
Reproduced with permission from the Wiley Publishers from Ref. [34].

replaced. For terpyridine (trpy) complexes similar photoinduced ligand exchange reactions involving monodentate ligands have been observed including a report by McMillin and coworkers [33] for the compound $[Ru(tpy)(bpy)CH_3CN)]^{2+}$.

Photoinduced ligand loss has been used to design molecular motors driven by thermal and photochemical stimuli as shown by Sauvage and co-workers [34]. A typical example of such a system is shown in Fig. 2 where replacement of a catenane ligand by chloride anions is observed when photolysis is carried out in $CH_2Cl_2$ in the presence of $Et_4NCl$. This process leads to a free but still connected catenane ring and the photoinduced arrangement can be reversed by thermal means.

Rhenium carbonyl complexes are of interest as photocatalytic centres for the reduction of $CO_2$ and a detailed understanding of the photochemical properties of such compounds is of prime importance in determining the reaction mechanism in these catalytic processes. As a result the photocatalytic properties of rhenium complexes of the type *fac*-$[Re(bpy)(CO)_3L]^{n+}$ (for L = $Cl^-$, $CN^-$, $NCS^-$, $n = 0$ and when L = $PR_3$, $n = 1$) have been investigated in detail [19]. For rhenium complexes of the type *fac*-$[Re(X_2bpy)(CO)_3(PR_3)]^+$, where X is H, $CH_3$ or $CF_3$ and R = Ph, Et, N–Bu, O–i-Pr, OPh or OMe, CO loss is observed upon irradiation of the compounds in acetonitrile with 365 nm light. Isotopic experiments have shown that the CO ligand *trans* to the $PR_3$ group is selectively substituted (Fig. 3) [35].

The photolability observed for these compounds is explained by electronic properties similar to those shown for ruthenium polypyridyl complexes. Also for these compounds the $^3$MC state is implicated in the photoinduced ligand exchange. Population of this level at room temperature can occur thermally from the LUMO

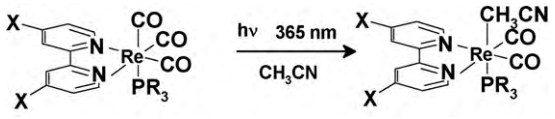

**Fig. 3.** Photoinduced CO loss upon irradiation at 365 nm of *fac*-$[Re(X_2bpy)(CO)_3(PR_3)]^+$.

$^3$MLCT state. The energy difference between the $^3$MLCT and the $^3$MC state in these rhenium compounds is between 3200 and 4800 $cm^{-1}$. These values are similar to those observed for compounds such as $[Ru(bpy)_3]^{2+}$ [36]. This photochemical lability of *fac*-$[Re(X_2bpy)(CO)_3(PR_3)]^+$ gives a novel and efficient synthetic pathway to complexes of the type *cis*,*trans*-$[Re(X_2bpy)(CO)_3(PR_3)]^{n+}$. On the other hand, *fac*-$[Re(bpy)(CO)_3(Cl)]$ is photostable at 365 nm. For this compound and for the corresponding pyridine derivative *fac*-$[Re(bpy)(CO)_3(pyridine)]^+$, the temperature dependence of the emission lifetime is small with an activation energy of around 250 $cm^{-1}$. This is considerably lower than observed for *fac*-$[Re(X_2bpy)(CO)_3(PR_3)]^+$. The reason for the different behaviour observed for these compounds is not yet fully understood. The authors postulate that population of the $^3$MC state also occurs for the chloride and pyridine complexes. However, it is worth pointing out that small activation energies such as those observed for the rhenium–phosphine complexes have in the case of ruthenium polypyridyl compounds been associated with population of $^3$MCLT states rather than $^3$MC levels [36a].

Against the background of these results it is interesting to consider the mechanism for $CO_2$ reduction recently proposed by

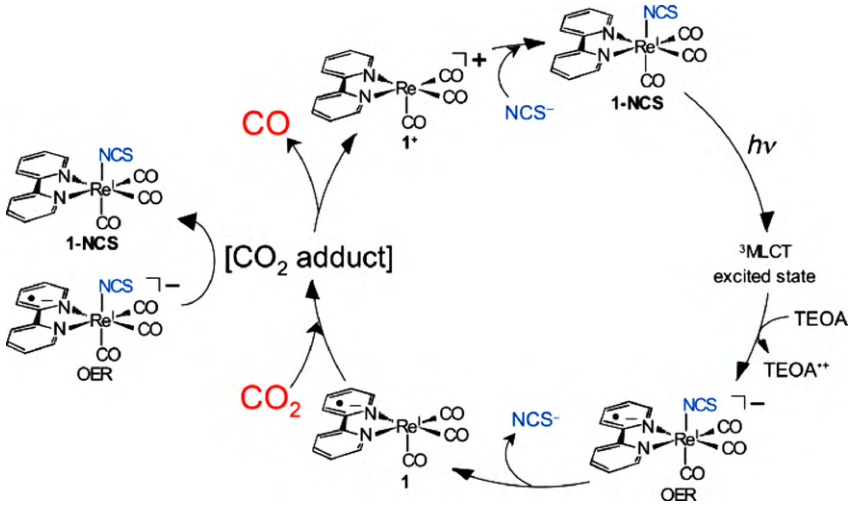


**Fig. 4.** Reaction mechanism for photocatalytic reduction of $CO_2$ to CO using *fac*-$[Re(bpy)(CO)_3NCS]$ as photocatalyst.
Reproduced with permission of the American Chemical Society from Ref. [19a].

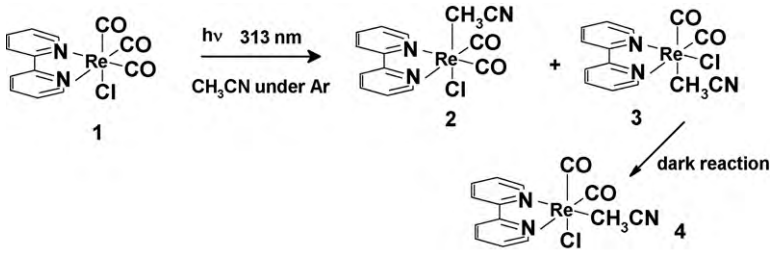


**Fig. 5.** Photoinduced and thermal processes observed upon irradiation of *fac*-[Re(bpy)(CO)$_3$Cl] at 313 nm.

Ishitani and co-workers [19] as shown in Fig. 4, in particular the nature of the one-electron reduced species (OER).

Since the $NCS^-$ complex like the related *fac*-[Re(bpy)(CO)$_3$Cl] is photostable at 365 nm, the anion is lost only after the excited state is reduced by the sacrificial agent. However, for the compound *fac*-[Re(bpy)(CO)$_3$(P(OEt)$_3$)]$^+$, loss of CO *trans* to the phosphine ligand has been reported. Since the latter compound shows a higher efficiency for $CO_2$ reduction than the $NCS^-$ species the question arises whether this loss of CO is reflected in the OER process and whether this behaviour is the reason for the improved performance of this system, in comparison to other known complexes reported.

While *fac*-[Re(bpy)(CO)$_3$Cl] is photostable at 365 nm the compound does show loss of CO to form *fac*-[Re(bpy)(CO)$_2$(CH$_3$CN)Cl] upon irradiation at 313 nm [37]. Photodissociation occurs on the subpicosecond time scale and is thought to occur via the $^1$MLCT state rather than the triplet state. Careful analysis of the reaction mixture, using X-ray analysis and NMR and IR spectroscopies show the presence of two main products, namely compounds **2** and **4** in Fig. 5. Compound **4** is a thermal product formed from the initial photoproduct **3**. This photochemical process provides a novel synthetic pathway towards rhenium dicarbonyl complexes.

## 3. Photoinduced isomerisation within the coordination sphere

One of the earliest isomerisations involving ruthenium polypyridyl complexes was reported by Meyer and co-workers. This group reported on the photoinduced *cis–trans* isomerisation of [Ru(bpy)$_2$(H$_2$O)$_2$]$^{2+}$ [38]. Upon irradiation of the *cis* compound by visible light the *trans* species is formed as confirmed by X-ray crystallography. The quantum yields for *cis–trans* and *trans–cis* isomerisations are independent of wavelength with values of 0.045 and 0.025, respectively and a photostationary state is observed upon extended photoplysis. Thermal *trans–cis* isomerisation is also observed.

Metal complexes containing three asymmetric ligands can in principle form facial (*fac*) and meridional (*mer*) isomers. Such isomers are observed for Ir-based cyclometalated complexes, with ligands such as 2-phenylpyridine, and 1-phenylpyrazole. These compounds are very promising as components in OLED devices and hence their photophysical properties have been investigated in great detail with *fac*-[Ir(CN̂)$_3$] isomers having considerably stronger emission than the corresponding *mer*-isomers [39,40]. The complexes can be prepared by thermal methods and depending on the temperature the *fac*- (high temperature) or *mer*-isomers (low temperature) are obtained. However, *mer*- to *fac*-isomerisation can also be carried out by irradiation with UV light [39] as shown in Fig. 6.

The photochemical behaviour of optically pure samples has also been investigated. Starting from the *mer*-Δ isomer, both Δ and Λ species of the *fac*-isomers are obtained, however the *mer*-Λ isomer is not observed [41]. These observations are in agreement with the strong emission observed for the *fac* isomer and the very weak signal observed for the *mer* species. For the latter, non-radiative processes are clearly important and limit the efficiency of the emission process.

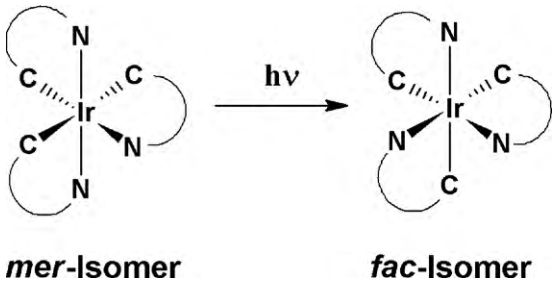


**Fig. 6.** Photoinduced *mer*/*fac* isomerisation in cyclometallated iridium complexes.

For the earlier mentioned compound *fac*-[Re(bpy)(CO)$_3$Cl] *fac*- to *mer*-isomerisation is also observed. Upon irradiation at 313 nm under a CO atmosphere in a non-coordinating solvent the *mer*-isomer is obtained in a 33% yield [42] (Fig. 7).

## 4. Photoinduced linkage isomerisation/chelate formation

There is considerable interest in linkage isomerisation of dimethyl sulfoxide (DMSO) when attached to ruthenium polypyridyl complexes. Compounds such as [Ru(bpy)(tpy)(DMSO)]$^{2+}$ and [Ru(bpy)$_2$(DMSO)$_2$]$^{2+}$ are typical examples. A review of the photoinduced isomerisation of such compounds has recently appeared [23b]. The photolability of these ligands has been exploited to gain access to enantiomerically pure ruthenium complexes of the type [Ru(bpy)$_2$(DMSO)Cl]$^+$ [43]. The ground and excited state properties of [Ru(bpy)(tpy)(DMSO)]$^{2+}$ have been studied together with the isomerisation process using time-dependent DFT [44].

Several studies have been carried out on the photophysics and photochemistry of ruthenium polypyridyl complexes containing 1,2,4-triazole moieties such as 3-(pyridine-2-yl)-1,2,4-triazole (Hpytr). These ligands are of interest since they are asymmetric, the nitrogen atoms in the triazole ring have different properties which may lead to the formation of different coordination isomers. In addition, the triazole N–H proton is quite acidic and this allows for the synthesis of complexes containing either protonated or deprotonated triazole rings [45]. For these complexes photoinduced linkage isomerisation processes are observed including photochemical photo/thermal reversible transformations. Importantly, triazolato compounds of the type [Ru(bpy)$_2$(pytr$^-$)]$^+$ are photostable. This is related to the strong sigma donor capacity of the deprotonated triazole ring. This leads to a considerable increase

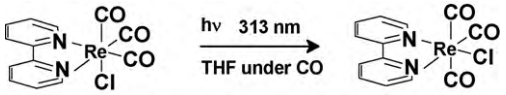


**Fig. 7.** *fac*- to *mer*-isomerisation for *fac*-[Re(bpy)(CO)$_3$Cl].

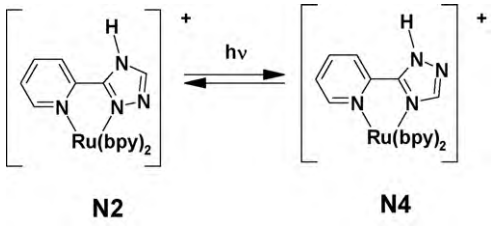


**Fig. 8.** Reversible photoinduced N2–N4 isomerisation of $[Ru(bpy)_2(Hpytr)]^{2+}$.

in the energy of the deactivating $^3$MC level (Fig. 1) and the $^3$MC level cannot be populated from the LUMO at room temperature [45,46]. However, for complexes containing protonated or methylated triazole ligands the $^3$MC level is lowered, population at room temperature takes place and as a result photoinduced ligand rearrangements are observed for such compounds. The first example is based on the $[Ru(bpy)_2(Hpytr)]^{2+}$ complex. As shown the complex is protonated and is therefore photoactive. For this complex two different isomers can be obtained, the Hpytr ligand is bound via either the N2 or N4 nitrogen atom of the triazole ring as shown in Fig. 8. For the unsubstituted triazole ring the ratio between these two isomers is 1:1 and they can be isolated by semi-preparative HPLC. Irradiation of either the N2 or N4 isomer in $CH_2Cl_2$ with visible light leads to a photostationary state with a N4:N2 ratio of 4:1. This ratio is in agreement with the activation energies observed for population of the $^3$MC state of the N4 and N2 species which show values of 2860 and 1710 $cm^{-1}$, respectively [46].

The second example involves a complex of the type $[Ru(bpy)_2(1Mepytr)]^{2+}$ (Fig. 9) [47]. This compound was obtained by direct methylation of the N2 isomer shown in Fig. 8 [48]. Methylation is observed at the N1 nitrogen of the triazole ring, a position not expected when considering steric considerations, but explained by the more electron negative nature of N1 compared to N4. Irradiation in acetonitrile leads to a very fast rearrangement leading to the sterically preferred configuration as shown in Fig. 9. This process is not reversible and can be followed conveniently in acetone by $^1$H NMR by monitoring the position of the methyl group as shown in Fig. 10. Upon photolysis in acetone the location of the methyl group changes dramatically from being close to neighbouring bpy ligands to a more free position, this process is reflected in the change of the resonance for this group from about 3.60 to 4.20 ppm.

In the last example photolysis of the 4-methyl analogue $[Ru(bpy)_2(4Mepytr)]^{2+}$ (Fig. 11) leads to the formation of a monodentate intermediate in high yield [49]. The photochemical process can be reversed by heating as shown in Figs. 11 and 12. A kinetic analysis shows that the thermal reaction follows first order kinetics with a rate constant of $(2 \pm 0.2) \times 10^{-4}\ s^{-1}$ at 80 °C. An activation energy for the reaction of $110 \pm 10\ kJ\ mol^{-1}$ was calculated over the temperature range 70–88 °C, while the entropy change is close to zero. Importantly, however, when the photoproduct obtained in acetonitrile is isolated and photolysed in either acetone or methanol the starting material is obtained. This suggests that in weakly coordinating solvents such as methanol and acetone photoinduced ring closure is observed.

Another example of a photoinduced ligand rearrangement is that shown in Fig. 13 [50]. Irradiation of a ruthenium containing macrocycle shown results in ligand rearrangement where the phenanthroline part of the macrocycle is rotated by 90°. As a result the pyridine ligand occupies a different position with respect to the mesityl group. This rearrangement is confirmed by NMR using NOESY which shows interactions between the pyridine group and the phenanthroline ligand in the starting material and pyridine mesityl interaction for the photoproduct. For these compounds, thermal reactions aimed at replacement of the monodentate ligand do, in general, lead to retention of the photoinduced geometry. In this manner complexes can be prepared which cannot be obtained by thermal methods. Note therefore that the addition of trifluoroacetic acid is required to change the connectivity observed for the photoproduct to that of the thermally obtained starting material.

Kojima and Fukuzumi reported similar photoinduced rearrangements for complexes based on the ligand tris(2-pyridylmethyl)amine (TPA) as shown in Fig. 14 [51].

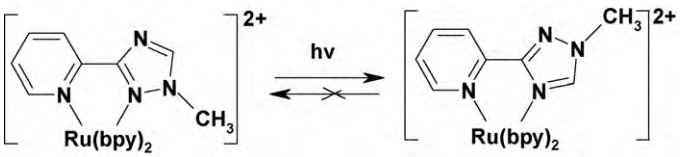


**Fig. 9.** Photoinduced irreversible N2 to N4 isomerisation for $[Ru(bpy)_2(1Mepytr)]^{2+}$.

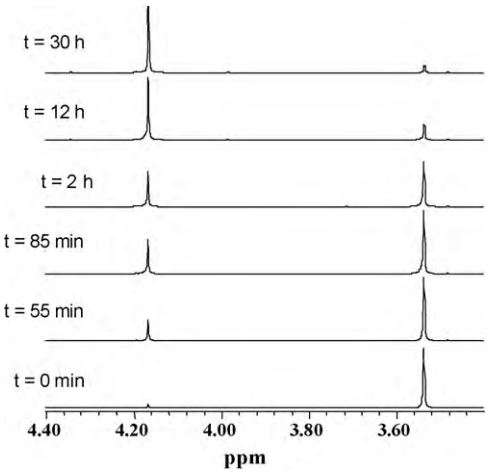


**Fig. 10.** $^1$H NMR spectra taken during photolysis of N2 to N4 isomer in $d_6$-acetone. Reproduced with permission from Wiley Publishers from Ref. [47].

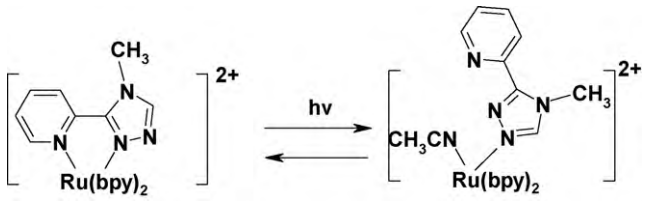


**Fig. 11.** Reversible photochemical/thermal linkage isomerisation for $[Ru(bpy)_2(4Mepytr)]^{2+}$.

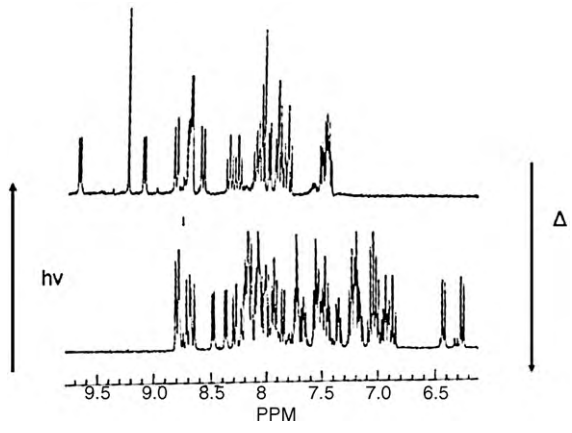


**Fig. 12.** $^1$H NMR spectra illustrating the photochemical/thermal rearrangements shown in Fig. 11.

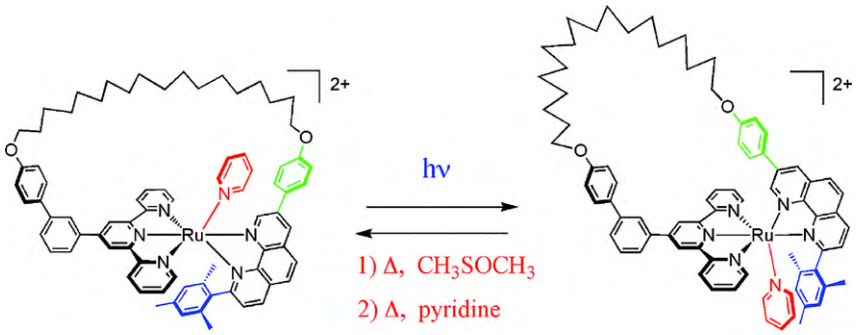


**Fig. 13.** Reversible photochemical/thermal ligand rearrangement ruthenium compound incorporating a catenane type ligand. Reproduced with permission from American Chemical Society from Ref. [50].

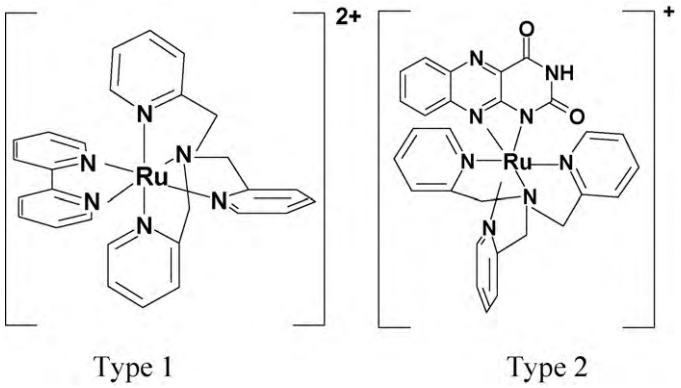


**Fig. 14.** TPA based metal complexes.

For type I compounds, intermediates containing pendant pyridine groups can be formed by either thermal or photoinduced processes. In a detailed study the formation of the intermediates is investigated and the nature of the products observed and the quantum yields for the photoprocesses for forward and backward reactions are reported. In acetonitrile the thermal process is irreversible and is taking place via an associative process. However, by a combination of thermal and photoinduced processes a 90% reversibility of the structural changes observed can be achieved. For type 2 compounds a photochemically induced isomerisation of the alloxazine ligand is observed. This rearrangement can be reversed by thermal means (Fig. 15).

Linkage isomerisation is also common in organometallic complexes and ultrafast processes relevant to photoinduced linkage isomerisation in organometallic systems were recently reviewed [52]. Burkey and co-workers have shown that the 1st row organometallic complexes of manganese, ($\eta^5$-$C_5H_4CH_3$)$Mn(CO)_2$(L) with non-chelatable bifunctional ligands (L)

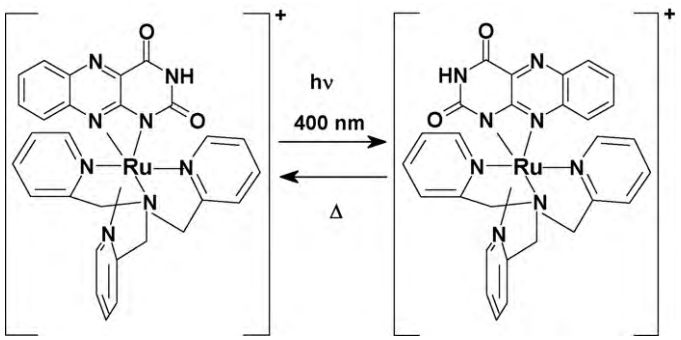


**Fig. 15.** Reversibly photochemical/thermal ligand rearrangements.

undergo linkage isomerisation, following irradiation as shown in Fig. 16. These results demonstrate that linkage isomerisation is an effective photochromatic mechanism for organometallic complexes. NMR, UV–vis and IR spectroscopy were used to monitor isomerisation, which occurred by both unimolecular and bimolecular processes, depending on the ligand (L) [53].

Ring formation in $CpMn(CO)_3$ (cp = cyclopentadienyl) derivatives with pendant sulphides have more recently been investigated as possible systems for ultrafast photoswitches [54]. $CpMn(CO)_3$ derivatives were chosen because of the high quantum yield (0.65) for photosubstitution of a carbonyl ligand. The pendant sulfides chosen are shown in Fig. 17. For the pendant $-CH_2SMe$ (**1**) ligand, a unit quantum yield for chelation was measured *albeit* via a secondary pathway involving formation of a solvated intermediate (solvent = heptane) [55]. Chelation competed with solvation of the unsaturated manganese centre on the picosecond time scale, which led initially to a 1:1 ratio of the chelate to solvated intermediate. The solvated intermediate is unstable and yields the chelate within 100 ns. Unfortunately solvation impedes the response time for chelation. In an attempt to prevent formation of the solvated intermediate pendant bis and tri derivatives were studied. Similar to the monomethylsulfide, the pendant methylsulfides gave rise to both the chelate and the solvated intermediate (1:1 ratio). The solvated intermediate ring closed with 200 ns. However, in the case of the pendant trimethylsulfide only the chelate was observed within 100 ps. These studies have demonstrated that relatively small conformational changes can exclude ultrafast processes such as solvation (in hexane) and furthermore clearly demonstrate that cage processes such as recombination and solvation can be problematic in designing organometallic photoswitches.

Subsequent picosecond infrared studies were carried out on the sulfide manganese tricarbonyl complexes **1**–**3** (Fig. 17), with results clearly demonstrating that the solvent employed influenced the reaction pathway [56]. For instance, in heptane there is competition between chelation (Mn–S) and solvent (S) coordination on the picosecond time scale, with the solvated intermediate forming the chelate on the nanosecond time base. However, when acetonitrile is employed as solvent the chelate forms within 13 ps, with no evidence for the solvated species. The presence of a chelating

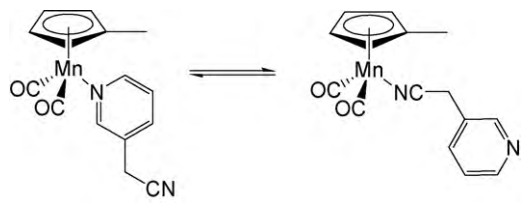

**Fig. 16.** Linkage isomerisation in ($\eta^5$-$C_5H_4CH_3$)$(CO)_2$L type complexes (where L = 3-cyanomethylpyridine).

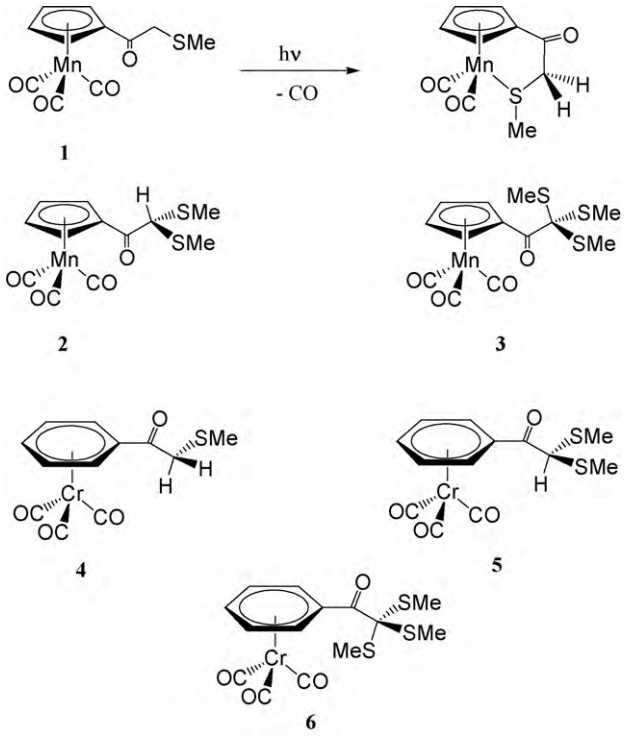


**Fig. 17.** Cyclopenadienyl $Mn(CO)_3$ and arene chromium tricarbonyl derivatives with mono-, di- and tri-pendant sulfides.

side chain may preclude solvation. Excitation of **1** or **2** at 289 nm in acetonitrile leads to CO loss, with formation of the chelate (Mn–S) complex, which differs from that in heptane where only the solvated intermediate was observed.

The influences of solvent and pendant substituent on the chelation dynamics for a series of arene chromium tricarbonyl complexes (**4**–**6**, Fig. 17) were also studied using TRIR [57]. In heptane all chromium complexes yielded both the Cr–S chelate and Cr–heptane solvated intermediate following excitation at 289 nm, in varying ratios (1:2, 1:2, 2:1 respectively for complexes **4**, **5** and **6**). Similar to the manganese systems discussed above, in all cases the Cr–heptane solvated species converted to the chelate within 30 ns. On changing the solvent to THF, again both the Cr–S chelate and Cr–THF species were observed for **2** and **3** following excitation, with the THF adducts converting to the chelate on the second time scale. In contrast to the manganese systems, in acetonitrile all three chromium complexes yielded the Cr–$NCCH_3$ species within 50 ps.

## 5. Photoinduced *cis–trans* rearrangements

Photoinduced ligand-based isomerisations such as *cis–trans* and locked/unlocked processes for spiropyrans have been studied for a wide range of metals. Rhenium carbonyl polypyridine complexes have attracted attention in recent years because these chromophores can be incorporated into catalytic systems for $CO_2$ reduction, conducting polymers and molecular wires, in addition to being attached to proteins and a host of others. Such systems, particularly those with stilbene-type ligands attached may act as molecular photonic devices due to photonic properties. In some rhenium polypyridine (N–N) complexes of $[Re(CO)_3(N–N)(L)]$ (L = axial ligand) the lowest excited state is localised on the ligand L, and if populated will result in isomerisation. Coordination of stilbene-type ligands to metals centres such as rhenium has the advantage of MLCT tunability over their organic counterparts, which opens up the possibility of using visible light for the isomerisation process. Iha and co-workers [58] have investigated the photoisomerisation of the trans-L ligand in the compounds *fac*-$[Re(Me_4\text{-phen})(CO)_3(\text{trans-L})]^+$ where trans-L is 1,2-bis(4-pyridyl)ethyne (bpe) or 4-styrene pyridine(stpy). Upon irradiation of *fac*-$[Re(Me_4\text{-phen})(CO)_3(\text{trans-L})]^+$ with UV light a *trans-cis* isomerisation of the olefin ligand is observed as shown in Fig. 18.

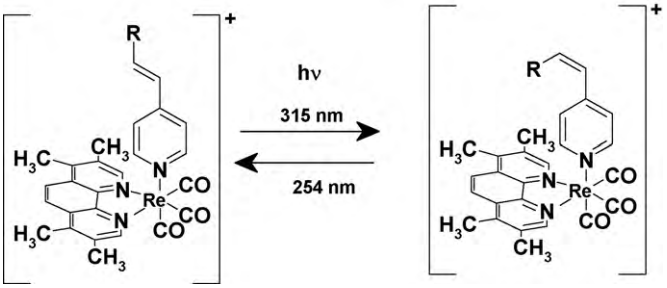


**Fig. 18.** *trans–cis* isomerisation of stpy type ligand in *fac*-$[Re(Me_4\text{-phen})(CO)_3(stpy)]^+$.

Upon irradiation of the *trans* isomer at 313, 334, 365 and 405 nm the *cis* compound is reformed. The isomerisation process can be reversed for both the stpy and the bpe compounds upon irradiation at 254 nm with a quantum yield of 0.15. Interestingly the *cis* complexes emit at room temperature and the emission spectrum obtained can be explained by a dual emission involving $^3IL_{phen}$ and $^3MLCT_{Re\rightarrow phen}$ emitting states. An investigation of the electronic spectra of the complexes suggests that the $^3IL_{trans\text{-}L}$ state is lowest in energy and therefore the isomerisation process is postulated to occur by population of that energy level. Quantum yields for *trans–cis* isomerisation are also reported for the bpe containing compound and values around 0.30 are obtained. For the stpy compound the quantum yield at 404 nm is similar at 0.35 but at higher energy irradiation values of about 0.55 are obtained. The authors interpret this observation by proposing that for the bpe complex population of the $^3IL_{trans\text{-}L}$ state occurs via internal conversion from the $^3$MLCT level at all wavelengths. However, for the stpy compound direct population from the $^1IL_{trans\text{-}L}$ states is occurring also at higher energies, yielding to higher overall quantum yields. The isomerisation of the bpe ligand is furthermore confirmed by time resolved absorption and infrared measurements carried out on complexes containing the non-substituted phen ligand [58c]. These measurements indicate the presence of an intermediate species with a lifetime of 28 ns. The investigation of the $\nu$(C=C) region of the spectrum suggests that this species observed is most likely the olefin localised twisted triplet $3p^*$ excited state.

In a related study the excited state dynamics of $[Re(Cl)(CO)_3(MeDpe^+)_2]^{2+}$ and $[Re(MeDpe^+)(CO)_3(bpy)]^{2+}$ ($MeDpe^+$ = *N*-methyl-4-[*trans*-2-(4-pyridyl)ethenyl]pyridinium, bpy = 2,2′-bipyridine), have recently been reported by Vlček and co-workers [59]. These studies have clearly demonstrated how subtle structural changes can lead to different excited state behaviour and lack of photoisomerisation in the case of $[Re(Cl)(CO)_3(MeDpe^+)_2]^{2+}$. Excitation (400 nm) of $[Re(MeDpe^+)(CO)_3(bpy)]^{2+}$ leads to population of two excited states, $Re(CO)_3 \rightarrow MeDpe^+$ and $Re(CO)_3 \rightarrow bpy$ $^3$MLCT states, from which a $MeDpe^+$ localised intraligand $^3\pi\pi^*$ excited state ($^3$IL) is populated over ~0.6 and ~10 ps. The *cis* isomer is produced from the $^3$IL state. In the case of the $[Re(Cl)(CO)_3(MeDpe^+)_2]^{2+}$ complex the lowest excited state is assigned to a $Re(Cl)(CO)_3 \rightarrow MeDpe^+$ $^3$MLCT. This state decays to the ground state with lifetimes of ~42 and 430 ps, thus the system is photostable (Fig. 19).

An overview of the excited state deactivation pathways for both systems is presented in Fig. 20. As is clearly evident from

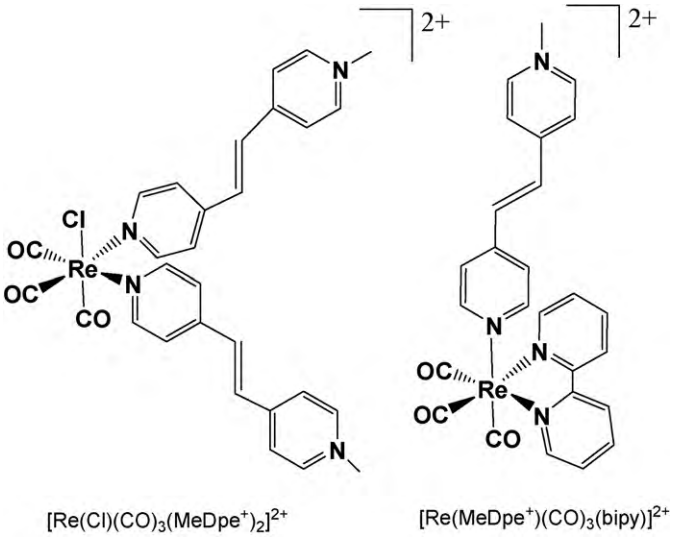


**Fig. 19.** $[Re(Cl)(CO)_3(MeDpe^+)_2]^{2+}$ and $[Re(MeDpe^+)(CO)_3(bpy)]^{2+}$.

these two schemes, the excited state behaviour in the photochemistry is caused by the different order in the excited states. For the $[Re(Cl)(CO)_3(MeDpe^+)_2]^{2+}$ complex, the $^3$MLCT(MeDpe$^+$) state is unreactive and decays to the ground state via electron transfer ($MeDpe^- \rightarrow Re^{II}$). Optical excitation of $[Re(MeDpe^+)(CO)_3(bpy)]^{2+}$ leads initially to population of $^3$MLCT states, however these are not the lowest excited states. The $^3$IL state lies lower in energy

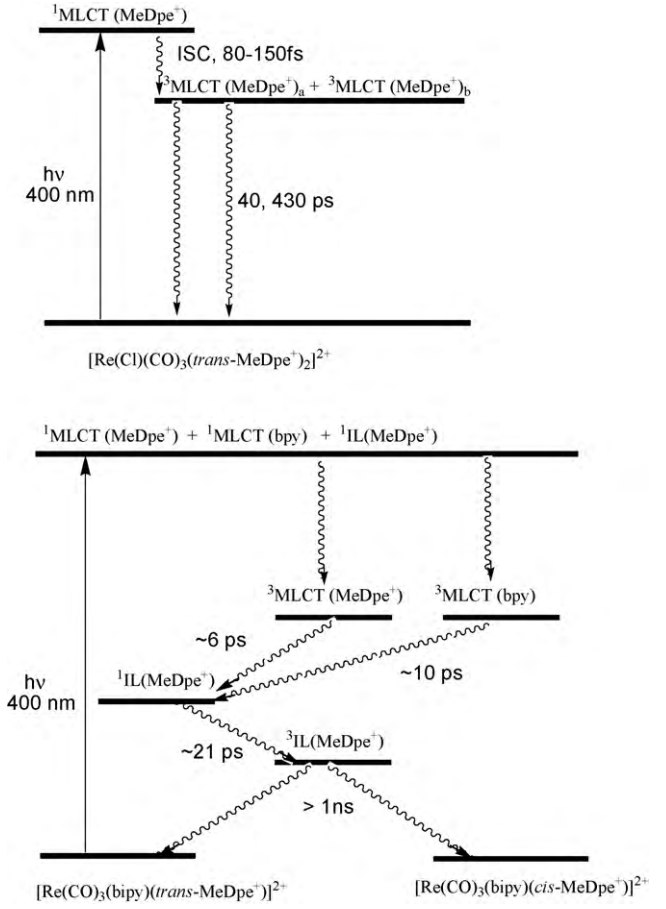


**Fig. 20.** Proposed mechanism for deactivation for both $[Re(Cl)(CO)_3(MeDpe^+)_2]^{2+}$ and $[Re(MeDpe^+)(CO)_3(bpy)]^{2+}$. The subscripts a and b denote two $^3$MLCT states of similar origin.

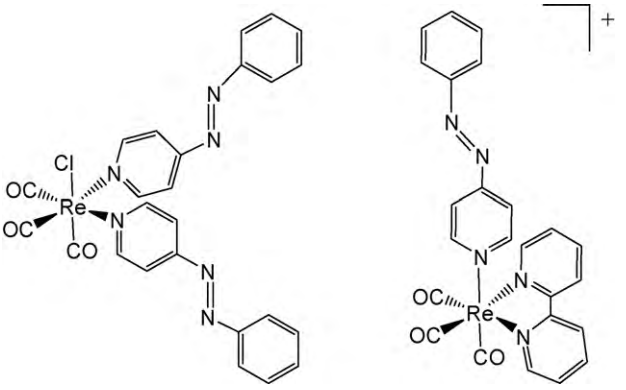

**Fig. 21.** Structures of *fac*-$[Re(Cl)(CO)_3(papy)_2]$ and *fac*-$[Re(papy)(CO)_3(bpy)]^+$.

and is thus populated by both $^3$MLCT(MeDpe$^+$) and $^3$MLCT(bpy) states.

The related azobenzene-type systems, *fac*-$[Re(Cl)(CO)_3(papy)_2]$ and *fac*-$[Re(papy)(CO)_3(bpy)]^+$ (papy = *trans*-4-phenylazopyridine) were also investigated using ultrafast techniques [60] (Fig. 21). UV irradiation results in *trans–cis* isomerisation for both complexes. The lowest excited state in both *fac*-$[Re(Cl)(CO)_3(papy)_2]$ and *fac*-$[Re(papy)(CO)_3(bpy)]^+$ is assigned to the $^3n\pi^*$ IL state of the papy ligand, however in these complexes the pathway for population of this state differs for the two complexes. Excitation at 400 nm leads to population of both $^1\pi\pi^*$(papy) and $^1$MLCT(papy) excited states, which subsequently undergo intersystem crossing to the $^3n\pi^*$ state. However for *fac*-$[Re(papy)(CO)_3(bpy)]^+$ the $^1\pi\pi^*$(papy), $^1$MLCT(papy) and, possibly also the $^1$MLCT(bpy) undergo branched intersystem crossing which populates both the $^3n\pi^*$ and $^3$MLCT(bpy) states within 0.8 ps. Previously photoisomerisation of azobenzene in metal complexes was attributed to an intraligand $^1n\pi^*$ excited state of the azobenzene moiety, as opposed to the $^3n\pi^*$ state observed by Vlcek et al. Hence these results show that coordination of rhenium to *trans*-4-phenylazopyridine switched *trans–cis* isomerisation from the singlet to the triplet excited state. Both rhenium complexes are examples of optically controlled switches as only the *cis* form is emissive and forms upon photoisomerisation. The latter study compliments a previous study based on the compounds *fac*-$[Re(Cl)(CO)_3(stpy)_2]$ and *fac*-$[Re(stpy)(CO)_3(bpy)]^+$ (stpy = *t*-4-styrylpyridine) (Fig. 22) [61]. Coordination of *trans*-4-styrylpyridine with the rhenium centre switches the *trans–cis* isomerisation mechanism from a singlet to a triplet $\pi\pi^*$ excited state. Thus rhenium acts as an intramolecular triplet sensitiser. The Re → stpy MLCT excited states are not involved in isomerisation. The isomerisation process in the papy complexes described above is approximately 200 times faster than that in the corresponding stpy complexes.

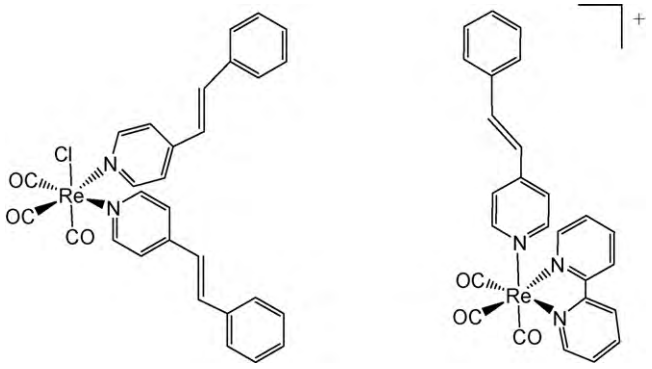

**Fig. 22.** Structures of *fac*-$[Re(Cl)(CO)_3(stpy)_2]$ and *fac*-$[Re(stpy)(CO)_3(bpy)]^+$.

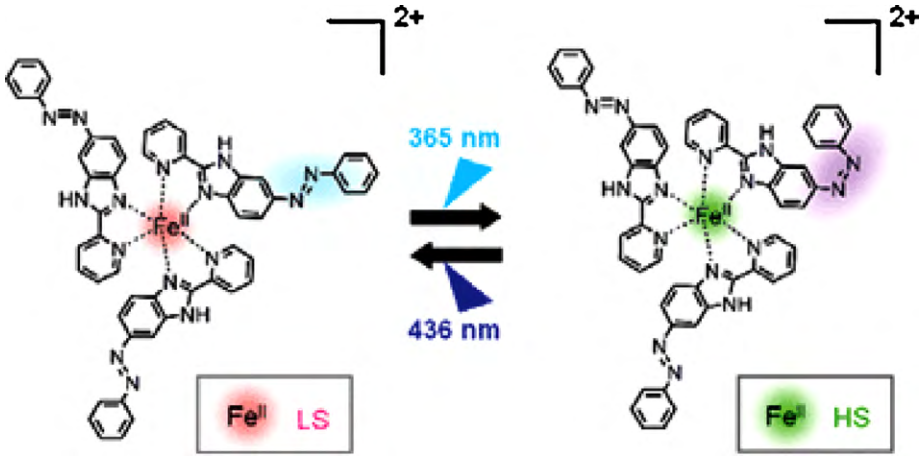


**Fig. 23.** Light driven spin change for by isomerisation of azobenzene containing ligand. Reproduced with permission from the Royal Society of Chemistry from Ref. [62].

A similar photoinduced *cis–trans* isomerisation has been reported for a Fe(II) complex [62] containing an azobenzene moiety attached to the pyridylbenzimidazole chelating ligand. Upon irradiation in acetone at room temperature the *cis* analogue can be produced by irradiation of the *trans* analogue at 365 nm. The process can be reversed by irradiation with 436 nm light as shown in Fig. 23. Interestingly while the *trans* isomer is low spin the *cis* species is high spin.

*Cis–trans* isomerisation in stilbene occurs efficiently using 313 nm irradiation. However, attachment of a $Cr(CO)_3$ moiety to one of the benzene rings in *cis*-stilbene has shown that the complex, *cis*-($\eta^6$-stilbene)$Cr(CO)_3$ efficiently undergoes photoisomerisation to the *trans* isomer following irradiation with $\lambda_{exc.} > 400$ [63]. Isomerisation in *cis*-($\eta^6$-stilbene)$Cr(CO)_3$ was clearly demonstrated by both matrix isolation studies with UV–vis and NMR experiments. The typical CO loss photoproduct, ($\eta^6$-stilbene)$Cr(CO)_2$ was observed following high-energy photolysis of *cis*-($\eta^6$-1,2-stilbene)$Cr(CO)_3$. Whether this CO loss occurs directly from the *cis*-isomer or by way of secondary photolysis of the initially produced *trans*-($\eta^6$-stilbene)$Cr(CO)_3$ is uncertain. More recently the photochemistry of both *cis*- and *trans*-($\eta^6$-stilbene)$Cr(CO)_3$ was probed using picosecond time resolved infrared and femtosecond transient absorption studies [64]. Three excited states were detected following excitation of *cis*-($\eta^6$-stilbene)$Cr(CO)_3$ at 400 nm. A short-lived excited state results in a fast *cis* to *trans* isomerisation (over 4 ps) of the coordinated stilbene in *cis*-($\eta^6$-stilbene)$Cr(CO)_3$, to yield the trans isomer *trans*-($\eta^6$-stilbene)$Cr(CO)_3$. The corresponding excited state in the *trans*-($\eta^6$-stilbene)$Cr(CO)_3$ failed to produce a significant yield of the *cis*-isomer. Of the remaining two excited states, one reacts to release one CO ligand while the second relaxes to the ground state. An overview of the photochemical pathways is depicted in Fig. 24.

Another type of photoinduced rearrangement includes haptotropic shifts at the ligand. Haptotropic shifts have been proposed for many organometallic reactions, in particular for thermally induced rearrangements [65], and to a lesser extent for photochemical reactions. Photoinduced changes to the coordination mode of π-bound ligands offer the possibility of opening up a number of coordination sites at the metal that may mimic the vacant site available on metal atoms in heterogeneous catalytic systems. Both matrix isolation studies at low temperature (12 K) and time resolved studies have facilitated the detection of inter-

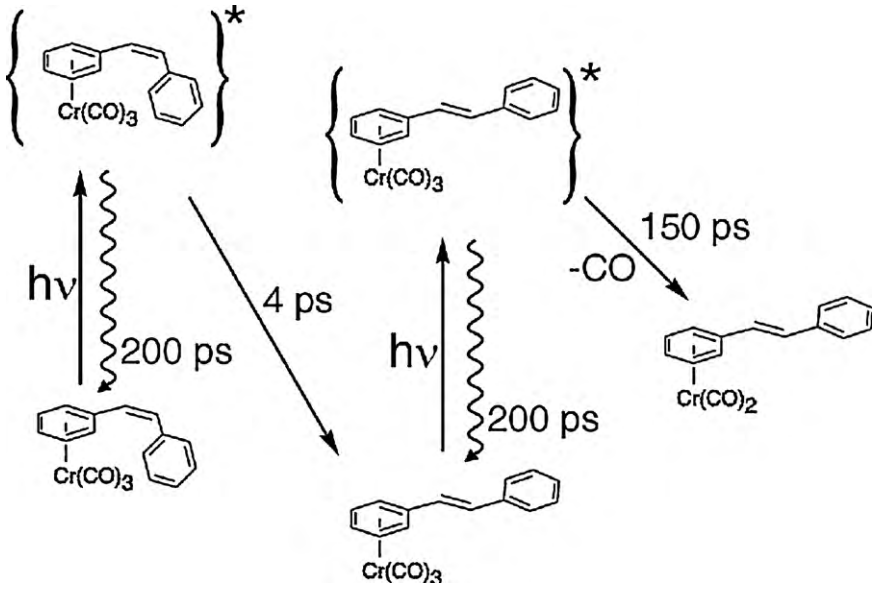


**Fig. 24.** Various intermediates and photoproducts observed following irradiation of *cis* and *trans* ($\eta^6$-stilbene)$Cr(CO)_3$.

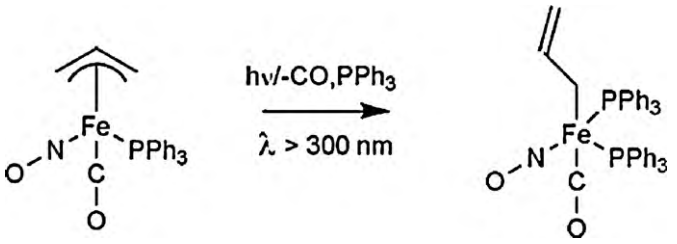


**Fig. 25.** $(\eta^3\text{-}C_3H_5)Fe(CO)(NO)(PPh_3)$ and $(\eta^1\text{-}C_3H_5)Fe(CO)(NO)(PPh_3)^2$.

mediates involving hapticity changes, where the electron count at the metal is less than 18. Recent examples that we have studied include organometallic complexes of Cr and Fe. In the case of $(\eta^6\text{-pyridine})Cr(CO)_3$, irradiation (460 nm) of the compound at 12 K, led to depletion of the parent bands together with the formation of infrared bands at 1957, 1841 and 1833 $cm^{-1}$ in a methane matrix, which are indicative of a *fac*-$Cr(CO)_3$ moiety [66]. Irradiation at higher energy (308 nm), yielded additional bands at 1945 and 1888 $cm^{-1}$. The latter bands were assigned to the CO loss photoproduct, $(\eta^6\text{-pyidine})Cr(CO)_2$, with the bands at 1957, 1841 and 1833 $cm^{-1}$ assigned to $(\eta^1\text{-pyridine})Cr(CO)_3$. The presence of two $N_2$ stretching vibrations (2222 and 2189 $cm^{-1}$) in a dinitrogen matrix confirmed two vacant sites at the metal centre, and thus in a dinitrogen matrix $(\eta^1\text{-pyidine})Cr(CO)_2(N_2)$ forms. Low energy photolysis gives rise only to the ring slip species, while higher energy gives rise to two photochemical pathways, thus wavelength dependent photochemistry exists. Time resolved studies using IR, also gave rise to bands assigned to the CO loss species. The lack of evidence for the ring slip intermediate at room temperature is attributed to rapid generation of $(\eta^6\text{-pyridine})Cr(CO)_3$, from $(\eta^1\text{-pyridine})Cr(CO)_3$. Further evidence for a thermal hapticity change from $\eta^1 \rightarrow \eta^6$ comes from UV–vis laser flash photolysis studies, where the trace for the recovery of the $(\eta^6\text{-pyridine})Cr(CO)_3$ displays a biphasic profile, with the faster process attributed to the $\eta^1 \rightarrow \eta^6$ transformation.

Similar to the pyridine system, irradiation of $(\eta^5\text{-}C_5H_4N)Fe(\eta^5\text{-}C_5H_5)$ with $\lambda > 495$ nm in a CO doped matrix at 12 K, led to the formation of product bands assigned to $(\eta^5\text{-}C_5H_5)(\eta^1\text{-}C_5H_4N)Fe(CO)$ and $(\eta^5\text{-}C_5H_5)(\eta^1\text{-}C_5H_4N)Fe(CO)_2$ [67]. Irradiation with monochromatic light (532 nm) produced a further product assigned to *exo*-$(\eta^5\text{-}C_5H_5)(\eta^3\text{-C-}C_5H_4N)Fe(CO)$. An additional monocarbonyl species was also observed which may be either an *endo*- or aza-allyl species. In solution studies at room temperature, photolysis of CO purged solutions of $(\eta^5\text{-}C_5H_4N)Fe(\eta^5\text{-}C_5H_5)$ gave rise only to formation of $(\eta^5\text{-}C_5H_5)(\eta^1\text{-}C_5H_4N)Fe(CO)_2$. Surprisingly, the ring slip intermediates observed following irradiation of azaferrocene appear only to interact with CO. Thermally $(\eta^5\text{-}C_5H_5)(\eta^1\text{-}C_5H_4N)Fe(CO)_2$ is converted to $(\eta^5\text{-}C_5H_5)Fe(\eta^5\text{-}C_5H_4N)$ [68]. Another iron system studied was $(\eta^3\text{-}C_3H_5)Fe(CO)(NO)(PPh_3)$ [69]. Irradiation ($\lambda > 300$ nm) of a cyclohexane solution of $(\eta^3\text{-}C_3H_5)Fe(CO)(NO)(PPh_3)$ in the presence of excess triphenylphosphine led to the production of infrared bands that were assigned to the haptotropic shift product $(\eta^1\text{-}C_3H_5)Fe(CO)(NO)(PPh_3)_2$ (Fig. 25), where the mode of coordination of the allyl ligand changes from $\eta^3 \rightarrow \eta^1$.

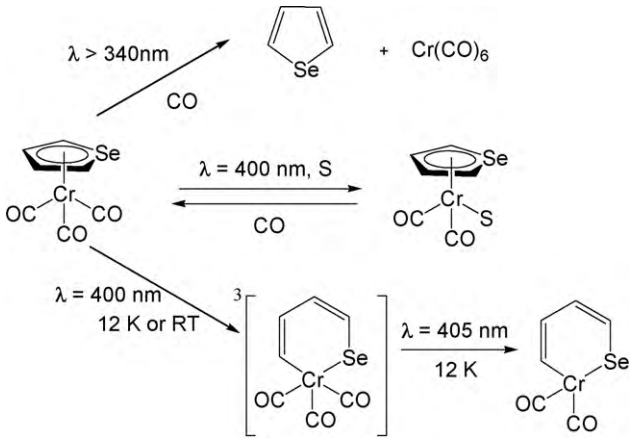


**Fig. 26.** Various reaction pathways available to $(\eta^5\text{-}C_5H_5Se)Cr(CO)_3$ following irradiation.

More recently we have studied the photochemical behaviour of $(\eta^5\text{-}C_5H_5Se)Cr(CO)_3$, using a combination of spectroscopic techniques at room and low temperature [70]. Low energy excitation (405 nm), in a matrix at 12 K induced an opening of the selenophene ring, with insertion of chromium into the Se–C, to form (C,*Se*–$C_5H_5Se)Cr(CO)_3$ initially. Further irradiation of this matrix led to formation of the CO loss product (C,*Se*–$C_5H_5Se)Cr(CO)_2$. Time resolved studies in heptane, with an excitation wavelength of 400 nm, produced the typical solvated CO loss species $(\eta^5\text{-}C_5H_5Se)Cr(CO)_2$(heptane). This species reacted with CO, to regenerate the parent material with a second-order rate constant of $5.8 \times 10^6$ $dm^3$ $mol^{-1}$ $s^{-1}$. In addition to the solvated 16 electron intermediate, new product bands at 2039, 2014, 2000, 1959 and 1954 $cm^{-1}$, were assigned to both, the ring insertion photoproduct (C,*Se*–$C_5H_5Se)Cr(CO)_3$, and the corresponding CO loss

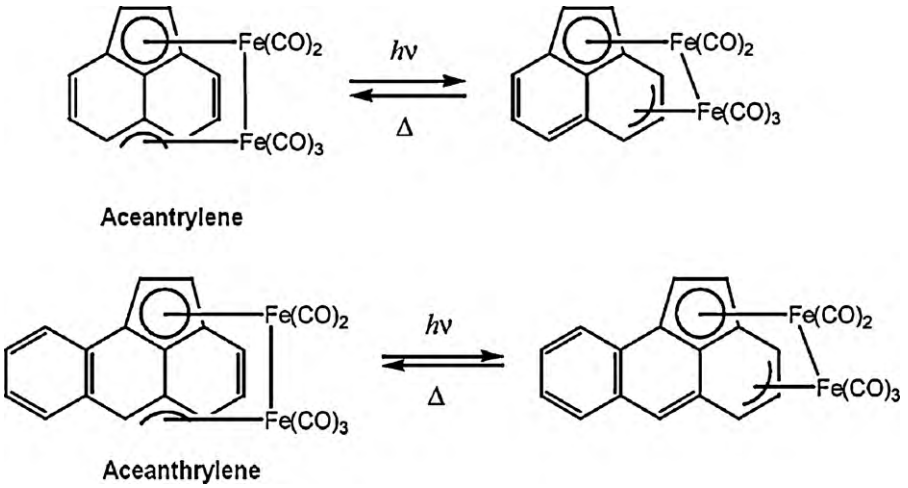


**Fig. 27.** $(\mu^2,\eta^3\text{:}\eta^5\text{-acenaphthylene})Fe_2(CO)_5$ and $(\mu^2,\eta^3\text{:}\eta^5\text{-aceanthrylene})Fe_2(CO)_5$.

product (C,*Se*–$C_5H_5Se$)$Cr(CO)_2$. Insertion of the chromium tricarbonyl fragment into the Se–C bond is complete within 1 ns. The insertion product does not appear to react with CO or $N_2$ in the matrix, and the unreactive nature of this coordinatively unsaturated intermediate is attributed to its triplet character. This study is the first example of photochemical insertion of a $Cr(CO)_3$ moiety into a carbon–heteroatom bond, to generate a chromaselenabenzene species (Fig. 26).

Nagashima and co-workers have shown that di-iron complexes bound to either acenaphthylene or aceanthrylene ligands thermally undergo reversible photoisomerisation both in solution and in the solid state [71]. In solution both complexes ($\mu^2,\eta^3{:}\eta^5$-acenaphthylene)$Fe_2(CO)_5$ and ($\mu^2,\eta^3{:}\eta^5$-aceanthrylene)$Fe_2(CO)_5$ following irradiation at 600 nm undergo a induced haptrotopic rearrangement to form the less stable isomer. For both complexes, a wavelength dependency for isomerisation was observed with higher energy irradiation leading to lower ratios for the thermodynamically less stable isomer. The quantum yields for the photochemically generated isomers were determined as $\Phi = 0.30$ and $\Phi = 0.013$ for the ($\mu^2,\eta^3{:}\eta^5$-acenaphthylene)$Fe_2(CO)_5$ and ($\mu^2,\eta^3{:}\eta^5$-aceanthrylene)$Fe_2(CO)_5$ complexes, respectively. The isomerisation quantum yield for the acenaphthylene complex is significantly higher than that for the aceanthrylene. Solid-state studies were carried out in KBr pellets, with reversible interconversions observed, over 10 repeat cycles. Changes were observed by monitoring the infrared spectra. These results elegantly demonstrate that organometallic photochromism in the solid state is detectable using IR light (Fig. 27).

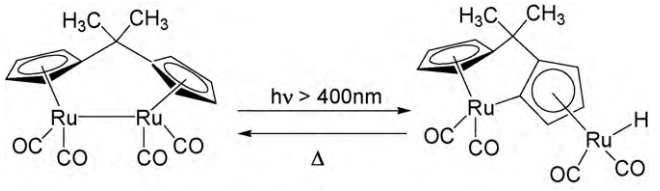


**Fig. 28.** The $CMe_2$ bridged dicyclopentadienyl diruthenium complex [$Me_2C(\eta^5$-$C_5H_4)_2Ru_2(CO)_4$].

Burger [72] reported that the $CMe_2$ bridged dicyclopentadienyl diruthenium complex [$Me_2C(\eta^5$-$C_5H_4)_2Ru_2(CO)_4$] acts as a reversible organometallic thermo-optical switch. When toluene or benzene solutions of the ruthenium complex were irradiated with $\lambda > 400$ nm, the system quantitatively and efficiently rearranged to the metal hydride as shown in Fig. 28. This transformation led to cleavage of a C–H bond on a cyclopentadienyl ring together with rupture of the Ru–Ru bond. Homolysis of the Ru–Ru bond was suggested as the first step in the rearrangement process. High temperatures of up to 160 °C were required to thermally reverse the reaction in the solid sate. This clearly indicates a much higher free enthalpy for the reverse reaction, which is thermally induced.

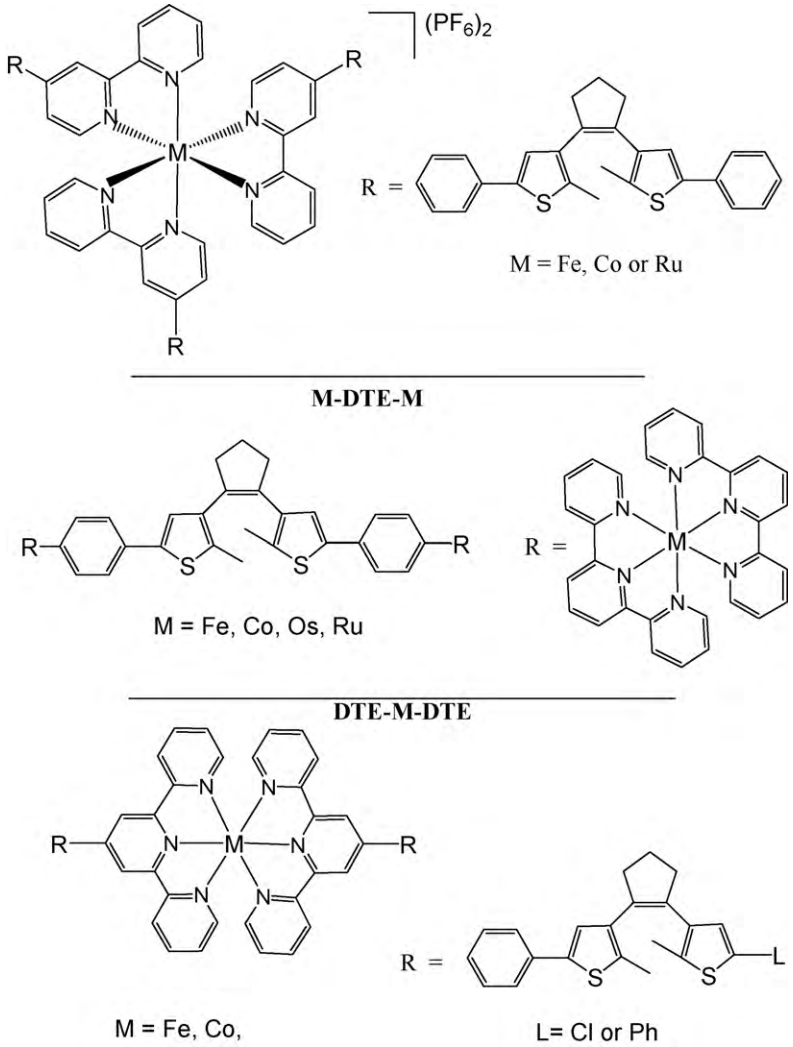


**Fig. 29.** Dithienylethene complexes.

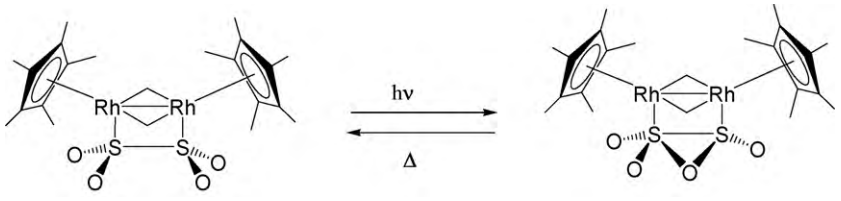


**Fig. 30.** Structures for $[(RhCp^*)_2(\mu\text{-}CH_2)_2(\mu\text{-}O_2SSO_2)]$ and $[(RhCp^*)_2(\mu\text{-}CH_2)_2(\mu\text{-}O_2SOSO)]$.

Organic photochromic molecules, particularly diarylethenes have extensively been studied for their use as photochromic materials [73]. Dithienyl ethenes interconvert photochemically between the non-conjugated 'open' form and the conjugated 'closed' form using specific wavelengths, and as a result are one of the most intensively studied systems [74]. In recent years redox-active centres containing transition metals have been tethered to dithienyl ethenes. These complexes have been reported for their ability to control electron transfer, switching luminescence or metal–metal communication [75]. As this area has grown extensively in recent years only a representative number of recent publications will be discussed here.

The photophysical and electrochemical properties of a series of linear and star-shaped molecules composed of transition metal bipyridines and dicyclopentenes have been studied by Abruña and co-workers [76]. Interestingly the photochromic behaviour was dependent on both the metal ($Fe^{II}$, $Co^{II}$, $Ru^{II}$ or $Os^{II}$) and the arrangement of various components. For instance in the star-shaped $Co^{II}$ and $Fe^{II}$ tethered dicyclopentenes shown in Fig. 29, photoisomerisation occurs following irradiation with 350 nm. In the case of the $Fe^{II}$ complex approximately 8 h irradiation was required to reach the photostationary state, whereas after only 10 min irradiation, the $Co^{II}$ complex quickly transformed into the closed form. One possibility for the dramatic difference in photoactivity for these two systems, is that in the case of the $Fe^{II}$ analogue, energy transfer from the dithienylethene to the $^3$MC or $^3$MLCT states may occur (a band in the UV–vis spectrum at 543 nm is assigned to a MLCT transition). In the case of the $Co^{II}$ analogue, no such MLCT transition is obvious in the UV–vis spectrum. The star shaped $Ru^{II}$ analogue also differs from $Fe^{II}$ or $Co^{II}$ systems, in so far as photoisomerisation can occur by irradiating either the dithienylethene band at 350 nm or the MLCT band at 470 nm. Irradiation of the latter most likely results in intramolecular energy transfer from the $^3$MLCT to the dithienylethene centred triplet state. In the case of the linear molecules shown in Fig. 29, the DTE-M-DTE arrangements (only Cl substituted $Fe^{II}$ system photoinactive) display superior photochromic behaviour when compared to the M-DTE-M arrangement ($Fe^{II}$, $Ru^{II}$ and $Os^{II}$ photoinactive). In addition to a difference in photoactivity with the metal centre, substituents such as Cl or a phenyl group also have a significant effect on photochromic behaviour, with the Cl leading generally to a decrease in photoactivity.

Other organometallic moieties linked to dithienylethenes include σ-bonded redox-active organometallic units such as $M(\eta^5\text{-}C_5H_4R)L_2$ where M = Fe or Ru and L = $(CO)_2$, $(CO)(PPh_3)$ or dppe, or where the organometallic moiety is attached via C≡C linkers for instance $[Fe(\eta^5\text{-}C_5Me_5)(dppe)_2]$ [77]. In this example, the Ru systems underwent photocyclisation more efficiently than the corresponding Fe analogues, while attaching a phosphine ligand impedes cyclisation. Attachment of the dppe ligand resulted in no photoactivity regardless of the metal centre in the σ-bonded redox-active organometallic units. Interestingly when C≡C linkers are employed, the dithienylethenes containing a dppe group formed the ring closed product following irradiation.

Recent studies have shown that the rhodium dinuclear complex $[(RhCp^*)_2(\mu\text{-}CH_2)_2(\mu\text{-}O_2SSO_2)]$ ($Cp^*$ = pentamethylcyclopentadienyl) interconverts quantitatively to $[(RhCp^*)_2(\mu\text{-}CH_2)_2(\mu\text{-}O_2SOSO)]$ [78]. This reaction is triggered by absorption of 510 nm light into the charge-transfer band from σ(S–S) to σ*(S–S) and σ*(Rh–Rh) orbitals, Fig. 30.

Studies on the organorhodium dithionate complex discussed here represent one of the few examples of photochromic crystals based on metal complexes. Furthermore, most photochromic materials involve photocyclisation, *cis*/*trans* isomerisation, or H transfer, but the rhodium system differs in that it involves intramolecular oxygen-atom insertion.

## 6. Concluding remarks and future developments

In this overview a wide range of photoinduced processes for both organometallic compounds and transition metal complexes are discussed. The processes observed vary from photoinduced ligand exchange, to photoinduced isomerisation of the coordination sphere and isomerisation of the ligands attached and ligand rearrangements. Where appropriate the relevance of the photochemical transformations for catalytic processes such as the water gas shift reaction and photocatalytic $CO_2$ reduction is outlined. However, more studies are required to improve our understanding of the relationship between photochemical transformations and photocatalytic processes. These studies should involve both detailed photophysical and theoretical studies including DFT.

The application of the photoinduced modification of molecules for the development of molecular machines has been highlighted widely as already indicated in the introduction. It is generally accepted that the successful immobilisation of supramolecular assemblies of solid surfaces is an important requisite for the successful design of a practical device [79]. The most important step to realising practical applications may be related to the successful immobilisation of components on solid surfaces without deactivation of the photoprocesses of interest. This can be achieved when polymers modified with ruthenium complexes are mobilised on electrode surfaces. The photochemical properties of $[Ru(bpy)_2(PVI)Cl]Cl$ where PVI is poly N-vinyl imidazole [80] and $[Ru(bpy)_2(PVP)Cl]Cl$, where PVP is poly-4-vinylpyridine [81] have successfully been transferred from solution to electrode surfaces and the photolability of the Cl ligand can be utilised to modify the sensing selectivity of the modified electrode. More recently the unidirectional molecular motor reported by Feringa was also successfully transferred to a gold surface via thiol containing linkers while retaining its photochemically and thermally driven rearrangements [82]. Pseudorotaxanes have also been immobilised and reversible dethreading and rethreading have been observed indicating that molecular motion can also been retained at solid surfaces [83]. Other studies carried out have included the immobilisation of photoactive materials on nanoparticles [84] and carbon nanotubes [85]. Examples of photonic interfacial assemblies based on monolayers have also been discussed [86]. It is important to realise that the surface used for the immobilisation of the photoac-

tive components may have a strong effect on the photophysical properties of the attached molecules. A particularly important example of this is in the Grätzel type dye sensitised solar cell, where the inherent photolability of the attached dyes may be eliminated by the strong coupling between the molecules and the $TiO_2$ surface [5]. These examples demonstrate that the photophysical properties of photoactive compounds can be transferred to surfaces and in this manner novel interfacial assemblies can be obtained. Finally, a relatively long but underrepresented relationship exists between photophysics and magnetism. Gütlich and Goodwin [87] have carried out a considerable amount of excellent and detailed work on light induced excited state spin trapping, a process that is normally observed at low temperatures. In addition ligand driven light induced spin change has been observed at room temperature in solution as reported in by Nishihara and co-workers [62]. In a recent review novel developments in the area of nanomagnetic materials such as single molecule magnets have been reviewed [88]. With these novel materials in mind it seems likely that increased collaboration between the two research areas could lead to the development of optical/magnetic systems with unique and unexpected properties.

## Acknowledgements

The authors thank Science Foundation Ireland (Grant No. 07/SRC/B1160, Advanced Biomimetic Materials for Solar Energy Conversion and Grant numbers 08/RFP/CHE1349 and 05/RF/PHY082) and the Environmental Protection Agency (Project number 2008-ET-MS-3-S2) for financial support.

## References

[1] (a) A.W. Adamson, J. Phys. Chem. 77 (1967) 798;
(b) A.W. Adamson, Advances in Chemistry Series, No. 49, American Chemical Society, Washington, DC, 1965.
[2] L.G. Vanquickenborne, A. Ceulemans, J. Am. Chem. Soc. 99 (1977) 2208.
[3] (a) G. Sprintschnik, H.W. Sprintschnik, P.P. Kirsch, D.G. Whitten, J. Am. Chem. Soc. 98 (1976) 2337;
(b) G. Sprintschnik, H.W. Sprintschnik, P.P. Kirsch, D.G. Whitten, J. Am. Chem. Soc. 99 (1977) 4949.
[4] (a) V. Balzani, A. Juris, M. Venturi, S. Campagna, S. Serroni, Chem. Rev. 96 (1996) 759;
(b) L. De Cola, P. Belser, Coord. Chem. Rev. 177 (1998) 301;
(c) V. Balzani, F. Scandola, Supramolecular Photochemistry, Ellis Horwood, New York, 1991;
(d) J.G. Vos, J.M. Kelly, Dalton Trans. (2006) 4869.
[5] (a) B. O'Regan, M. Grätzel, Nature 353 (1991) 737;
(b) A. Hagfeldt, M. Grätzel, Acc. Chem. Res. 33 (2000) 269.
[6] (a) E. Baranoff, J.-H. Yum, M. Grätzel, Md.K. Nazeeruddin, J. Organomet. Chem. 694 (2009) 2661;
(b) L. Flamigni, J.-P. Collin, J.-P. Sauvage, Acc. Chem. Res. 41 (2008) 857;
(c) A. Coleman, C. Brennan, J.G. Vos, M.T. Pryce, Coord. Chem. Rev. 252 (2008) 2585;
(d) R.A. Kirgan, B.P. Sullivan, D.P. Rillema, Top. Curr. Chem. 281 (2007) 45;
(e) A. Vlček, S. Záliš, Coord. Chem. Rev. 251 (2007) 258;
(f) A.S. Polo, M.K. Itokazu, K.M. Frin, A.O. de Toledo Patrocínio, N.Y.M. Iha, Coord. Chem. Rev. 250 (2006) 1669.
[7] (a) Y. Degani, A. Heller, J. Am. Chem. Soc. 111 (1989) 2367;
(b) A. Heller, Acc. Chem. Res. 23 (1990) 128;
(c) A. Heller, J. Phys. Chem. 96 (1992) 3567;
(c) A. Aoki, A. Heller, J. Phys. Chem. 97 (1993) 11014;
(d) A.P. Doherty, M.A. Stanley, D. Leech, J.G. Vos, Anal. Chim. Acta 319 (1996) 111;
(e) A.P. Doherty, J.G. Vos, J. Chem. Soc., Faraday Trans. 88 (1992) 2903;
(f) A.P. Doherty, M.A. Stanley, J.G. Vos, Analyst 120 (1995) 2371.
[8] (a) T. Albrecht, A. Guckian, J. Ulstrup, J.G. Vos, Nano Lett. 5 (2005) 1451;
(b) T. Albrecht, A. Guckian, J. Ulstrup, J.G. Vos, IEEE Trans. Nanotechnol. 4 (2005) 430;
(c) T. Albrecht, K. Moth-Poulsen, J.B. Christensen, A. Guckian, T. Bjornholm, J.G. Vos, J. Ulstrup, Faraday Discuss. 131 (2006) 265;
(d) R. Bechman, K. Beverly, A. Boukai, Y. Bunimovich, J.W. Choi, E. DeIonno, J. Green, E. Johnston-Halperin, Y. Luo, B. Sheriff, J.F. Stoddart, J.R. Heath, Faraday Discuss. 131 (2006) 9.
[9] (a) C. Mallins, S. Fanni, H.G. Glever, J.G. Vos, B.D. MacCraith, Anal. Commun. 36 (1999) 3;
(b) A. Lobnik, I. Oehme, I. Murkovic, O.S. Wolfbeis, Anal. Chim. Acta 367 (1998) 159;
(c) J.N. Demas, B.A. DeGraff, J. Chem. Educ. 74 (1997) 690.
[10] (a) P.-T. Chou, Y. Chi, Chem. Eur. J. 13 (2007) 380;
(b) H. Inomata, K. Goushi, T. Masuko, T. Konno, T. Imai, H. Sasabe, J.J. Brown, C. Adachi, Chem. Mater. 16 (2004) 1285;
(c) H. Yamamoto, J. Wilkinson, J.P. Long, K. Bussman, J.A. Christodoulides, Z.H. Kafafi, Nano Lett. 5 (2005) 2485.
[11] (a) V. Balzani, Small 1 (2005) 278;
(b) V. Bazani, M. Venturi, A. Credo, Molecular Devices and Machines, Wiley-VCH, Weinheim, 2003;
(c) J.P. Sauvage, Acc. Chem. Res. 31 (1998) 611;
(d) J.P. Collin, V. Heitz, S. Bonnet, J.-P. Sauvage, Inorg. Chem. Commun. 8 (2005) 1063.
[12] (a) J.K. Barton, A.T. Danishefsky, J.M. Goldberg, J. Am. Chem. Soc. 106 (1984) 2172;
(b) J.K. Barton, J.M. Goldberg, C.V. Kumar, N.J. Turro, J. Am. Chem. Soc. 108 (1986) 2081.
[13] (a) J.M. Kelly, A.B. Tossi, D.J. McConnell, C. OhUigin, Nucleic Acids Res. 13 (1985) 6017;
(b) L. Jacquet, J.M. Kelly, A. Kirsch-De Mesmaeker, J. Chem. Soc., Chem. Commun. (1995) 913;
(c) L. Jacquet, R.J.H. Davies, A. Kirsch-De Mesmaeker, J.M. Kelly, J. Am. Chem. Soc. 119 (1997) 11763;
(d) L.M. Wilhelmsson, F. Westerlund, P. Lincoln, B. Norden, J. Am. Chem. Soc. 124 (2002) 12092.
[14] G. Steinberg-Yfrach, J.-L. Rigaud, E.N. Durantini, A.L. Moore, D. Gust, T.A. Moore, Nature 392 (1998) 479.
[15] N. Koumura, R.W.J. Zijlstra, R.A. van Delden, N. Harada, B.L. Feringa, Nature 401 (1999) 152.
[16] (a) N. Armaroli, V. Balzani, J.-P. Collin, P. Gavina, J.-P. Sauvage, B. Ventura, J. Am. Chem. Soc. 121 (1999) 4397;
(b) B. Champin, P. Mobian, J.-P. Sauvage, Chem. Soc. Rev. 36 (2007) 358;
(c) V. Balzani, M. Clemente-Leon, A. Credi, B. Ferrer, M. Venturi, A.H. Flood, J.F. Stoddart, Proc. Natl. Acad. Sci. U.S.A. 103 (2006) 1178;
(d) V. Balzani, G. Bergamini, P. Ceroni, Coord. Chem. Rev. 252 (2008) 2456.
[17] S. Rau, D. Walther, J.G. Vos, Dalton Trans. (2007) 915, and references therein.
[18] (a) S.W. Gersten, G.J. Samuels, T.J. Meyer, J. Am. Chem. Soc. 104 (1982) 4029;
(b) P. Doppelt, T.J. Meyer, Inorg. Chem. 26 (1987) 2027;
(c) O. Ishitani, P.S. White, T.J. Meyer, Inorg. Chem. 35 (1996) 2167;
(d) M. Yagi, A. Syouji, S. Yamada, M. Komi, H. Yamazaki, S. Tajima, Photochem. Photobiol. Sci. 8 (2009) 139.
[19] (a) H. Takeda, K. Koike, H. Inoue, O. Ishitani, J. Am. Chem. Soc. 130 (2008) 2023;
(b) Y. Hayashi, S. Kita, B.S. Brunschwig, E. Fujita, J. Am. Chem. Soc. 125 (2003) 11976;
(c) J. Hawecker, J.-M. Lehn, R. Ziessel, Helv. Chim. Acta 69 (1986) 1990;
(d) H. Takeda, O. Ishitani, Coord. Chem. Rev. 254 (2010) 346;
(e) E. Fujita, Coord. Chem. Rev. 185–186 (1999) 373;
(f) A.J. Morris, G.J. Meyer, E. Fujita, Acc. Chem. Res. 42 (2009) 1983.
[20] F.J. McQuillin, D.G. Parker, G.R. Stephenson, Transition Metal Organometallics for Organic Synthesis, Cambridge University Press, Cambridge, UK, 1991.
[21] (a) V.W.-W. Yam, C.-C. Ko, N.Y. Zhu, J. Am. Chem. Soc. 126 (2004) 12734;
(b) S. Kume, H. Nishihara, Dalton Trans. (2008) 3260;
(c) C.-C. Ko, W.-M. Kwok, V.W.W. Yam, D.L. Phillips, Chem. Eur. J. 12 (2006) 5840;
(d) M.N. Roberts, J.K. Nagle, J.G. Finden, N.R. Branda, M.O. Wolf, Inorg. Chem. 48 (2009) 19.
[22] (a) B.L. Feringa (Ed.), Molecular Switches, Wiley VCH, Weinheim, 2001;
(b) M.K.J. ter Wiel, R.A. van Delden, A. Meetsma, B.L. Feringa, J. Am. Chem. Soc. 127 (2005) 14208.
[23] P. Belser, S. Bernhard, C. Blum, A. Beyeler, L. De Cola, V. Balzani, Coord. Chem. Rev. 192 (1999) 155;
(b) J.J. Rack, Coord. Chem. Rev. 253 (2009) 78.
[24] (a) B.P. Sullivan, T.J. Meyer, Inorg. Chem. 21 (1982) 1037;
(b) B. Durham, J.V. Caspar, J.K. Nagle, T.J. Meyer, J. Am. Chem. Soc. 104 (1982) 4803;
(c) B. Durham, J.L. Walsh, C.L. Carter, T.J. Meyer, Inorg. Chem. 19 (1980) 860.
[25] S. Tachiyashiki, H. Ikezawa, K. Mizumachi, Inorg. Chem. 33 (1994) 623.
[26] J.M. Clear, J.M. Kelly, C.M. O'Connell, J.G. Vos, C.J. Cardin, S.R. Costa, A.J. Edwards, J. Chem. Soc., Chem. Commun. (1980) 750.
[27] J.M. Kelly, C.M. O'Connell, J.G. Vos, J. Chem. Soc., Dalton Trans. (1986) 253.
[28] (a) J.M. Kelly, J.G. Vos, Angew. Chem. Int. Ed. Engl. 94 (1982) 644;
(b) J.M. Kelly, J.G. Vos, J. Chem. Soc., Dalton Trans. (1986) 1045;
(c) J.G. Haasnoot, W. Hinrichs, O. Weir, J.G. Vos, Inorg. Chem. 25 (1986) 4140.
[29] J.-M. Lehn, R. Ziessel, J. Organomet. Chem. 382 (1990) 157.
[30] S. Chardon-Noblat, A. Deronzier, R. Ziessel, D. Zsoldos, J. Electrochem. Chem. 444 (1998) 253.
[31] (a) P.C. Ford, Acc. Chem. Res. 14 (1981) 31;
(b) H. Ishida, K. Tanaka, M. Morimoto, T. Tanaka, Organometallics 5 (1986) 724.
[32] B.E. Buchanan, E. McGovern, P. Harkin, J.G. Vos, Inorg. Chim. Acta 154 (1988).
[33] C.R. Hecker, P.E. Fanwick, D.R. McMillin, Inorg. Chem. 30 (1991) 659.
[34] P. Mobian, J.-M. Kern, J.-P. Sauvage, Angew. Chem. Int. Ed. 43 (2004) 2392.
[35] (a) K. Koike, N. Okoshi, H. Hori, K. Takeuchi, O. Ishitani, H. Tsubaki, I.P. Clark, M.W. George, F.P.A. Johnson, J.J. Turner, J. Am. Chem. Soc. 124 (2002) 11448;
(b) K. Koike, J. Tanabe, S. Toyama, H. Tsubaki, K. Sakamoto, J.R. Westwell, F.P.A. Johnson, H. Hori, H. Saitoh, O. Ishitani, Inorg. Chem. 39 (2000) 2777.

[36] (a) A. Juris, V. Balzani, F. Barigelletti, S. Campagna, P. Belser, A. von Zelewsky, Coord. Chem. Rev. 82 (1988) 85;
(b) T.J. Meyer, Pure Appl. Chem. 58 (1986) 1193;
(c) J. Davila, C.A. Bignozzi, F. Scandola, J. Phys. Chem. 93 (1989) 1373.
[37] S. Sato, A. Sekine, Y. Ohashi, O. Ishitani, A.M. Blanco-Rodrıguez, A. Vlcek Jr., T. Unno, K. Koike, Inorg. Chem. 46 (2007) 3531.
[38] B. Durham, S.R. Wilson, D.J. Hodgson, T.J. Meyer, J. Am. Chem. Soc. 102 (1980) 600.
[39] A.B. Tamayo, B.D. Alleyne, P.I. Djurovich, S. Lamansky, I. Tsyba, N.N. Ho, R. Bau, M.E. Thompson, J. Am. Chem. Soc. 125 (2003) 7377.
[40] T. Karatsu, E. Ito, S. Yagai, A. Kitamura, Chem. Phys. Lett. 424 (2006) 353.
[41] K. Tsuchiya, E. Ito, S. Yagai, A. Kitamura, T. Karatsu, Eur. J. Inorg. Chem. (2009) 2104.
[42] S. Sato, T. Morimoto, O. Ishitani, Inorg. Chem. 46 (2007) 9051.
[43] D. Hesek, G.A. Hembury, M.G.B. Drew, S. Taniguchi, Y. Inoue, J. Am. Chem. Soc. 122 (2000) 10236.
[44] I. Ciofini, C.A. Daul, C. Adamo, J. Phys. Chem. A 107 (2003) 11182.
[45] (a) R. Hage, J.G. Haasnoot, H.A. Nieuwenhuis, J. Reedijk, D.J.A. De Ridder, J.G. Vos, J. Am. Chem. Soc. 112 (1990) 9245;
(b) L. De Cola, F. Barigelletti, V. Balzani, R. Hage, J.G. Haasnoot, J. Reedijk, J.G. Vos, Chem. Phys. Lett. 178 (1991) 491;
(c) H.A. Nieuwenhuis, J.G. Haasnoot, R. Hage, J. Reedijk, T.L. Snoeck, D.J. Stufkens, J.G. Vos, Inorg. Chem. 30 (1991) 48;
(d) S. Fanni, T.E. Keyes, C.M. O'Connor, H. Hughes, R. Wang, J.G. Vos, Coord. Chem. Rev. 208 (2000) 77.
[46] R. Wang, J.G. Vos, R.H. Schmehl, R. Hage, J. Am. Chem. Soc. 114 (1992) 1964.
[47] S. Fanni, F.M. Weldon, L. Hammarström, E. Mukhtar, W.R. Browne, T.E. Keyes, J.G. Vos, Eur. J. Inorg. Chem. (2001) 529.
[48] S. Fanni, S. Murphy, J.S. Killeen, J.G. Vos, Inorg. Chem. 39 (2000) 1320.
[49] (a) B.E. Buchanan, H. Hughes, J. van Diemen, R. Hage, J.G. Haasnoot, J. Reedijk, J.G. Vos, J. Chem. Soc., Chem. Commun. (1991) 300;
(b) B.E. Buchanan, H. Hughes, P. Degn, J.M. Pavon Velasco, B.S. Creaven, C. Long, J.G. Vos, R.A. Howie, R. Hage, J.H. van Diemen, J.G. Haasnoot, J. Reedijk, J. Chem. Soc., Dalton Trans. (1992) 1177.
[50] S. Bonnet, J.-P. Collin, J.-P. Sauvage, Inorg. Chem. 46 (2007) 10520.
[51] (a) S. Miyazaki, T. Koyima, S. Fukuzumi, J. Am. Chem. Soc. 130 (2008) 1556;
(b) T. Koyima, T. Morimoto, T. Sakamoto, S. Miyazaki, S. Fukuzumi, Chem. Eur. J. 14 (2008) 8904.
[52] T.T. To, E.J. Heilweil, C.B. Duke, K.R. Ruddick, C.E. Webster, T.J. Burkey, J. Phys. Chem. A 113 (2009) 2666.
[53] T.T. To, C.E. Barnes, T.J. Burkey, Organometallics 23 (2004) 2708.
[54] J.S. Yeston, T.T. To, T.J. Burkey, E.J. Heilweil, J. Phys. Chem. B 108 (2004) 4582.
[55] T. Jiao, Z. Pang, T.J. Burkey, R.F. Johnson, T.A. Heimer, V.D. Kleiman, E.J. Heilweil, J. Am. Chem. Soc. 121 (1999) 4618.
[56] T.T. To, E.J. Heilweil, T.J. Burkey, J. Phys. Chem. A 110 (2006) 10669.
[57] T.T. To, E.J. Heilweil, C.B. Duke, T.J. Burkey, J. Phys. Chem. A 111 (2007) 6933.
[58] (a) A.O.T. Patrocinio, N.Y.M. Iha, Inorg. Chem. 47 (2008) 10851;
(b) K.P.M. Frin, K. Itokazu, N.Y.M. Iha, Inorg. Chim. Acta 363 (2010) 294;
(c) D.M. Dattelbaum, M.K. Itokazu, N.Y.M. Iha, T.J. Meyer, J. Phys. Chem. 107 (2003) 4092.
[59] M. Busby, F. Hartl, P. Matousek, M. Towrie, A. Vlček Jr., Chem. Eur. J. 14 (2008) 6912.
[60] M. Busby, P. Matousek, M. Towrie, A. Vlček Jr., Inorg. Chim. Acta 360 (2007) 885.
[61] M. Busby, P. Matousek, M. Towrie, A. Vlček Jr., J. Phys. Chem. A 109 (2005) 3000.
[62] Y. Hasegawa, S. Kume, H. Nishihara, Dalton Trans. (2009) 280.
[63] A.C. Coleman, S.M. Draper, C. Long, Conor, M.T. Pryce, Organometallics 26 (2007) 4128.
[64] A.C. Coleman, N.M. Boyle, C. Long, R. Augulis, A. Pugzlys, P.H.M. van Loosdrecht, W.R. Browne, B.L. Feringa, K.L. Ronayne, M.T. Pryce, Dalton Trans. 39 (2010) 229.
[65] Some representative examples of thermally induced haptotropic rearrangements:
(a) J.O.C. Jimenez-Halla, J. Robles, M. Sol, Organometallics 27 (2008) 5230;
(b) I.D. Gridnev, Coord. Chem. Rev. 252 (2008) 1798;
(c) Y. Oprunenko, S. Malyugina, A. Vasil'ko, K. Lyssenko, C. Elschenbroich, K. Harms, J. Organomet. Chem. 641 (2002) 208;
(d) K.H. Dotz, B. Wenzel, H.C. Jahr, Top. Curr. Chem. 248 (2004) 63;
(e) M.D. Fryzuk, L. Jafarpour, F.M. Kerton, J.B. Love, S.J. Rettig, Angew. Chem. Int. Ed. 39 (2000) 767.
[66] C.J. Breheny, S.M. Draper, F.-W. Grevels, W.E. Klozbucher, C. Long, M.T. Pryce, G. Russell, Organometallics 15 (1996) 3679.
[67] D.P. Heenan, C. Long, V. Montiel-Palma, R.N. Perutz, M.T. Pryce, Organometallics 19 (2000) 3869.
[68] J. Zakrzewski, C. Giannotti, J. Organomet. Chem. 388 (1990) 175.
[69] K. Maher, C. Long, M.T. Pryce, J. Organomet. Chem. 691 (2006) 3298.
[70] P. Brennan, M.W. George, O.S. Jina, C. Long, J. McKenna, M.T. Pryce, X.-Z. Sun, K.Q. Vuong, Organometallics 27 (2008) 3671.
[71] S. Niinayashi, K. Matsubara, M.-A. Haga, H. Nagashima, Organometallics 23 (2004) 635.
[72] P. Burger, Angew. Chem. Int. Ed. 40 (2001) 1917.
[73] (a) M.A. Garcia-Garibay, Angew. Chem. Int. Ed. 46 (2007) 8945;
(b) S. Kobatake, S. Takami, H. Muto, T. Ishikawa, M. Irie, Nature 446 (2007) 778;
(c) M. Irie, S. Kobatake, M. Horichi, Science 291 (2001) 1769.
[74] (a) M. Irie, Chem. Rev. 100 (2000) 1685;
(b) H. Tian, S. Yang, Chem. Soc. Rev. 33 (2004) 85.
[75] For some representative examples see the following:
(a) V. Aubert, V. Guerchais, E. Ishow, K. Hoang-Thi, I. Ledoux, K. Nakatani, H. Le Bozec, Angew. Chem. Int. Ed. 47 (2008) 577R;
(b) T.F. Jukes, V. Adamo, F. Hartl, P. Belser, L. De Cola, L. Coord, Chem. Rev. 249 (2005) 1327;
(c) J.K.-W. Lee, C.-C. Ko, K.M.-C. Wong, N. Zhu, W.-W. Yam, Organometallics 26 (2007) 12;
(d) T.-W. Ngan, C.-C. Ko, N. Zhu, N.W.-W. Yam, Inorg. Chem. 46 (2007) 1144;
(e) B. Qin, R. Yao, X. Zhao, H. Tian, Org. Biomol. Chem. 1 (2003) 2187;
(f) B. Qin, R. Yao, H. Tian, Inorg. Chim. Acta 357 (2004) 3382.
[76] (a) Y.-W. Zhong, N. Vila, J.C. Henderson, S. Flores-Torres, H.D. Abruña, Inorg. Chem. 48 (2009) 7080;
(b) Y.-W. Zhong, N. Vila, J.C. Henderson, S. Flores-Torres, H.D. Abruña, Inorg. Chem. 48 (2009) 991;
(c) Y.-W. Zhong, N. Vila, J.C. Henderson, S. Flores-Torres, H.D. Abruña, Inorg. Chem. 46 (2007) 10470.
[77] (a) Y. Tanaka, A. Inagaki, M. Akita, Chem. Commun. (2007) 1169;
(b) K. Motoyama, T. Koike, M. Akita, Chem. Commun. (2008) 5812.
[78] (a) H. Nakai, T. Nonaka, Y. Miyano, M. Mizuno, Y. Ozawa, K. Toriumi, N. Koga, T. Nishioka, M. Irie, K. Isobe, J. Am. Chem. Soc. 130 (2008) 17836;
(b) H. Nakai, M. Mizuno, T. Nishioka, N. Koga, K. Shiomi, Y. Miyano, M. Irie, B.K. Breedlove, I. Kinoshita, Y. Ozawa, K. Toriumi, T. Yonezawa, K. Isobe, Angew. Chem. Int. Ed. 45 (2006) 6473.
[79] (a) R.J. Forster, T.E. Keyes, J.G. Vos, Interfacial Supramolecular Assemblies, Wiley, Chichester, 2003;
(b) T. Kudernac, N. Katsonis, W.R. Browne, B.L. Feringa, J. Mater. Chem. 19 (2009) 7168;
(c) W.R. Browne, Coord. Chem. Rev. 252 (2008) 2470.
[80] S.M. Geraty, J.G. Vos, J. Electroanal. Chem. 176 (1984) 389.
[81] (a) J.M. Clear, J.M. Kelly, D.C. Pepper, J.G. Vos, Inorg. Chim. Acta 33 (1979) L139;
(b) O. Haas, M. Kriens, J.G. Vos, J. Am. Chem. Soc. 103 (1981) 1318;
(c) J.M. Clear, J.M. Kelly, C.M. O'Connell, J.G. Vos, J. Chem. Res. (M) (1981) 3039.
[82] (a) R.A. van Delden, M.K.L. ter Wiel, M.M. Pollard, J. Vicario, N. Koumura, B.L. Feringa, Nature 437 (2005) 1337;
(b) W.R. Browne, B.L. Feringa, Annu. Rev. Phys. Chem. 60 (2009) 407.
[83] (a) K. Kim, W.S. Jeon, J.-K. Kang, J.W. Lee, S.Y. Jon, T. Kim, K. Kim, Angew. Chem. Int. Ed. 42 (2003) 2293;
(b) S.Y. Chia, J.G. Cao, J.F. Stoddart, J.I. Zink, Angew. Chem. Int. Ed. 40 (2001) 2447.
[84] D.P. Ferris, Y.-L. Zhao, N.M. Khashab, H.A. Khatib, J.F. Stoddart, J.I. Zink, J. Am. Chem. Soc. 131 (2009) 1686.
[85] (b) Y-L. Zhao, L.B. Hu, G. Gruner, J.F. Stoddart, J. Am. Chem. Soc. 130 (2008) 16996;
(b) F. Frehill, J.G. Vos, S. Benrezzak, M. Rüther, W.J. Blau, A.I. Minett, A. Fonseca, J.B. Nagy, A. Koos, L. Birro, M. in het Panhuis, J. Am. Chem. Soc. 124 (2002) 13694.
[86] R.J. Forster, T.E. Keyes, Coord. Chem. Rev. 253 (2009) 1833.
[87] A.P. Gütlich, H.A. Goodwin, Top. Curr. Chem. 233 (2004) 1.
[88] S. Brooker, J.A. Kitchen, Dalton Trans. (2009) 7331.